ELECTRIC POWER
RESEARCH INSTITUTE

BWRVIP-169NP: BWR Vessel and Internals Project

Testing and Evaluation of BWR Supplemental Surveillance Program (SSP) Capsules A, B, and C

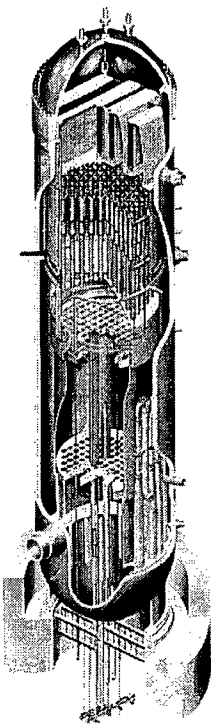

NON-PROPRIETARY INFORMATION

NOTICE: This report contains the non-proprietary information that is included in the proprietary version of this report. The proprietary version of this report contains proprietary information that is the intellectual property of BWRVIP utility members and EPRI. Accordingly, the proprietary report is available only under license from EPRI and may not be reproduced or disclosed, wholly or in part, by any Licensee to any other person or organization.

BWRVIP-169NP: BWR Vessel and Internals Project

Testing and Evaluation of BWR Supplemental Surveillance Program (SSP) Capsules A, B, and C

1013399NP

Final Report, March 2007

EPRI Project Manager
R. Carter

ELECTRIC POWER RESEARCH INSTITUTE
3420 Hillview Avenue, Palo Alto, California 94304-1338 • PO Box 10412, Palo Alto, California 94303-0813 • USA
800.313.3774 • 650.855.2121 • askepri@epri.com • www.epri.com

DISCLAIMER OF WARRANTIES AND LIMITATION OF LIABILITIES

THIS DOCUMENT WAS PREPARED BY THE ORGANIZATION(S) NAMED BELOW AS AN ACCOUNT OF WORK SPONSORED OR COSPONSORED BY THE BWR VESSEL AND INTERNALS PROJECT (BWRVIP) AND ELECTRIC POWER RESEARCH INSTITUTE, INC. (EPRI). NEITHER BWRVIP, EPRI, ANY MEMBER OF EPRI, ANY COSPONSOR, THE ORGANIZATION(S) BELOW, NOR ANY PERSON ACTING ON BEHALF OF ANY OF THEM:

(A) MAKES ANY WARRANTY OR REPRESENTATION WHATSOEVER, EXPRESS OR IMPLIED, (I) WITH RESPECT TO THE USE OF ANY INFORMATION, APPARATUS, METHOD, PROCESS, OR SIMILAR ITEM DISCLOSED IN THIS DOCUMENT, INCLUDING MERCHANTABILITY AND FITNESS FOR A PARTICULAR PURPOSE, OR (II) THAT SUCH USE DOES NOT INFRINGE ON OR INTERFERE WITH PRIVATELY OWNED RIGHTS, INCLUDING ANY PARTY'S INTELLECTUAL PROPERTY, OR (III) THAT THIS DOCUMENT IS SUITABLE TO ANY PARTICULAR USER'S CIRCUMSTANCE; OR

(B) ASSUMES RESPONSIBILITY FOR ANY DAMAGES OR OTHER LIABILITY WHATSOEVER (INCLUDING ANY CONSEQUENTIAL DAMAGES, EVEN IF BWRVIP, EPRI OR ANY EPRI REPRESENTATIVE HAS BEEN ADVISED OF THE POSSIBILITY OF SUCH DAMAGES) RESULTING FROM YOUR SELECTION OR USE OF THIS DOCUMENT OR ANY INFORMATION, APPARATUS, METHOD, PROCESS, OR SIMILAR ITEM DISCLOSED IN THIS DOCUMENT.

ORGANIZATION(S) THAT PREPARED THIS DOCUMENT

ATI Consulting

MPM Technologies, Inc.

TransWare Enterprises Inc.

NON-PROPRIETARY INFORMATION

NOTICE: This report contains the non-propriety information that is included in the proprietary version of this report. The proprietary version of this report contains proprietary information that is the intellectual property of BWRVIP utility members and EPRI. Accordingly, the proprietary report is available only under license from EPRI and may not be reproduced or disclosed, wholly or in part, by any Licensee to any other person or organization.

THE WORK DESCRIBED IN THIS REPORT WAS PREPARED, REVIEWED, ACCEPTED, AND ISSUED ACCORDING TO EPRI'S QUALITY ASSURANCE PROGRAM, WHICH COMPLIES WITH THE REQUIREMENTS OF TITLE 10 OF THE CODE OF FEDERAL REGULATIONS, PART 50, APPENDIX B.

NOTE

For further information about EPRI, call the EPRI Customer Assistance Center at 800.313.3774 or e-mail askepri@epri.com.

Electric Power Research Institute, EPRI, and TOGETHER...SHAPING THE FUTURE OF ELECTRICITY are registered service marks of the Electric Power Research Institute, Inc.

Copyright © 2007 Electric Power Research Institute, Inc. All rights reserved.

CITATIONS

This report was prepared by

ATI Consulting
P.O. Box 5769
24 Glenbarr Court
Pinehurst, NC 28374

Principal Investigators
T. Hardin
W. Server

MPM Technologies, Inc.
2161 Sandy Drive
State College, PA 16803

Principal Investigator
M. Manahan, Sr.

TransWare Enterprises Inc.
5450 Thornwood Dr., Suite M
San Jose, CA 95123

Principal Investigators
K Watkins
D. Jones

This report describes research sponsored by the Electric Power Research Institute (EPRI) and its BWRVIP participating members.

The report is a corporate document that should be cited in the literature in the following manner:

BWRVIP-169NP: BWR Vessel and Internals Project, Testing and Evaluation of BWR Supplemental Surveillance Program (SSP) Capsules A, B, and C. EPRI, Palo Alto, CA: 2007. 1013399NP.

PRODUCT DESCRIPTION

A Supplemental Surveillance Program (SSP) was developed in the early 1990s to gather additional surveillance data regarding the irradiation embrittlement of BWR vessel materials. In the late 1990s a BWR Vessel and Internals Project (BWRVIP) Integrated Surveillance Program (ISP) assumed responsibility for testing the SSP capsules for use in the integrated program. This report describes testing and evaluation of BWR Supplemental Surveillance Program (SSP) Capsules A, B, and C. These results will be used to monitor embrittlement as part of the BWRVIP ISP.

Results & Findings

The report includes specimen chemical compositions, capsule neutron exposure, specimen temperatures during irradiation, and Charpy V-notch test results. The project compared irradiated Charpy data for the specimens to unirradiated data to determine the shift in Charpy curves due to irradiation. Results indicate a shift lower than the predictions of Regulatory Guide 1.99, Revision 2, for seventeen of the twenty-four sets of material specimens. Flux wires were measured and fluence was determined for each specimen set within the three capsules.

Challenges & Objectives

Neutron irradiation exposure reduces the toughness of reactor vessel steel plates, welds, and forgings. The objectives of this project were two-fold:

- To document results of the neutron dosimetry and Charpy-V notch ductility tests for materials contained in the SSP capsules A, B, and C
- To compare results with the embrittlement trend prediction of U.S. Nuclear Regulatory Commission (USNRC) Regulatory Guide 1.99, Rev. 2.

Applications, Values & Use

Results of this work will be used in the BWRVIP ISP that integrates individual BWR surveillance programs into a single program. Data generated from the SSP specimens provide significant additional data of high quality to monitor BWR vessel embrittlement. The ISP and the use of the SSP capsule specimen data result in significant cost savings to the BWR fleet and provide more accurate monitoring of embrittlement in BWR vessels.

EPRI Perspective

The BWRVIP ISP represents a major enhancement to the process of monitoring embrittlement for the U.S. fleet of BWRs. The ISP optimizes surveillance capsule tests while at the same time maximizing the quantity and quality of data, thus resulting in a more cost effective program. The BWRVIP ISP provides more representative data that may be used to assess embrittlement in RPV vessel beltline materials and improve trend curves in the BWR range of irradiation conditions.

Approach

The project team inserted capsules into the Cooper reactor in November 1991 at a location of sufficient lead factor to provide the desired fluence. The team used dosimetry to gather information about the neutron fluence accrual of the specimens and placed thermal monitors in the capsules to approximate the highest temperature during irradiation. In March 2003, the team removed the capsules from the reactor and transported them to facilities for testing and evaluation. They performed a neutron transport calculation in accordance with Regulatory Guide 1.190 and compared to the results from the dosimetry. Testing of Charpy V-notch specimens were performed according to ASTM standards.

Keywords

Reactor pressure vessel integrity
Reactor vessel surveillance program
Radiation embrittlement
BWR
Charpy testing
Mechanical properties

CONTENTS

1 INTRODUCTION 1-1

1.1 Implementation Requirements 1-2

2 MATERIALS AND TEST SPECIMEN DESCRIPTION 2-1

2.1 Dosimeters 2-1

2.2 Thermal Monitors 2-1

2.3 Charpy V-Notch Specimens 2-6

2.3.1 Capsule Loading Inventory 2-6

2.3.2 Material Description 2-8

2.3.3 Chemical Composition 2-9

2.3.3 CVN Baseline Properties 2-12

2.4 Capsule Opening 2-15

2.4.1 Condition of Dosimeters 2-15

2.4.2 Condition of Thermal Monitors 2-16

3 NEUTRON FLUENCE CALCULATION 3-1

3.1 Description of the Reactor System 3-1

3.1.1 Reactor System Mechanical Design Inputs 3-1

3.1.2 Reactor System Material Compositions 3-2

3.1.3 Reactor Operating Data Inputs 3-4

3.1.3.1 Power History Data 3-4

3.1.3.2 Reactor State Point Data 3-4

3.1.3.3 Core Loading Pattern 3-5

3.2 Calculation Methodology 3-6

3.2.1 Description of the RAMA Fluence Methodology 3-6

3.2.2 The RAMA Geometry Model for Cooper Nuclear Station 3-7

3.2.3 RAMA Calculation Parameters 3-11

3.2.4 RAMA Neutron Source Calculation 3-11

3.2.5 RAMA Fission Spectra 3-11
3.2.6 Parametric Sensitivity Analyses 3-12
3.3 RAMA Nuclear Data Library 3-13
3.3.1 Nuclear Cross Sections 3-13
3.3.2 Activation Response Functions 3-14
3.4 Surveillance Capsule Activation Results 3-16
3.4.1 SSP Capsule A Activation Comparison Results 3-17
3.4.2 SSP Capsule B Activation Comparison Results 3-19
3.4.3 SSP Capsule C Activation Comparison Results 3-21
3.5 Surveillance Capsule Fluence Results 3-23
3.5.1 Surveillance Capsule Best Estimate Neutron Fluence and Flux for Energy >1.0 MeV 3-23
3.5.2 Surveillance Capsule Best Estimate Neutron Fluence and Flux for Energy >0.1 MeV 3-25

4 CHARPY TEST DATA 4-1
4.1 Charpy Test Procedure 4-1
4.2 Charpy Test Data 4-2

5 CHARPY TEST RESULTS 5-1
5.1 Analysis of Impact Test Results 5-1
5.2 Irradiated Versus Unirradiated CVN Properties 5-1

6 REFERENCES 6-1

A SUMMARY OF CHARPY V-NOTCH TEST DATA A-1

B TANH CURVE FIT PLOTS OF CVN TEST DATA B-1

C DOSIMETER ANALYSIS C-1
Dosimeter Material Description C-1
Dosimeter Cleaning and Mass Measurement C-1
Radiometric Analysis C-3

LIST OF FIGURES

Figure 2-1 Cooper SSP Capsule A 2-2
Figure 2-2 Cooper SSP Capsule B 2-3
Figure 2-3 Cooper SSP Capsule C 2-4
Figure 2-4 Cooper Nuclear Station SSP Capsule Holder 2-5
Figure 2-5 Schematic Representation of Thermal Monitor 2-6
Figure 2-6 Photograph of CNS Capsule A Wrapper Showing Indentations which Indicate that the Capsule was Irradiated with the Dosimetry Wires out of the Charpy Notches. 2-17
Figure 2-7 Photograph of CNS Capsule A Showing Fe and Cu Wires Out of the Charpy Notches. (Capsule U-Hook is at Top of Photograph) 2-18
Figure 2-8 Photograph of CNS Capsule B Showing Fe and Cu Wires Out of the Charpy Notches. (Capsule U-Hook is at Top of Photograph) 2-18
Figure 2-9 Photograph of CNS Capsule C Showing Fe and Cu Wires Out of the Charpy Notches. (Capsule U-Hook is at Top of Photograph) 2-19
Figure 3-1 Planar View of the Cooper Nuclear Station Reactor 3-2
Figure 3-2 Planar View of the Cooper Nuclear Station RAMA Model 3-8
Figure 3-3 Axial View of the Cooper Nuclear Station RAMA Model 3-10
Figure B-1 Charpy Energy Data for A1224-1 Grand Gulf Plate Unirradiated B-2
Figure B-2 Charpy Energy Data for A1224-1 Grand Gulf Plate Irradiated in Capsule A B-4
Figure B-3 Charpy Energy Data for A1224-1 Grand Gulf Plate Irradiated in Capsule B B-6
Figure B-4 Charpy Energy Data for C2331-2 Cooper Plate Unirradiated B-8
Figure B-5 Charpy Energy Data for C2331-2 Cooper Plate Irradiated in Capsule A B-10
Figure B-6 Charpy Energy Data for C2331-2 Cooper Plate Irradiated in Capsule B B-12
Figure B-7 Charpy Energy Data for P2130-2 Nine Mile Point 1 Plate Unirradiated B-14
Figure B-8 Charpy Energy Data for P2130-2 Nine Mile Point 1 Plate Irradiated in Capsule A B-16
Figure B-9 Charpy Energy Data for P2130-2 Nine Mile Point 1 Plate Irradiated in Capsule B B-18
Figure B-10 Charpy Energy Data for C3278-2 Fitzpatrick Plate Unirradiated B-20
Figure B-11 Charpy Energy Data for C3278-2 Fitzpatrick Plate Irradiated in Capsule A B-22
Figure B-12 Charpy Energy Data for C3278-2 Fitzpatrick Plate Irradiated in Capsule B B-24
Figure B-13 Charpy Energy Data for 5P6214B Grand Gulf Weld Unirradiated B-26
Figure B-14 Charpy Energy Data for 5P6214B Grand Gulf Weld Irradiated in Capsule A B-28

Figure B-15 Charpy Energy Data for 5P6214B Grand Gulf Weld Irradiated in Capsule B B-30
Figure B-16 Charpy Energy Data for 34B009 Millstone 1 Weld Unirradiated B-32
Figure B-17 Charpy Energy Data for 34B009 Millstone 1 Weld Irradiated in Capsule A B-34
Figure B-18 Charpy Energy Data for 34B009 Millstone 1 Weld Irradiated in Capsule B B-36
Figure B-19 Charpy Energy Data for AP2-21 Quad Cities 2 Weld Unirradiated B-38
Figure B-20 Charpy Energy Data for AP2-21 Quad Cities 2 Weld Irradiated in Capsule A B-40
Figure B-21 Charpy Energy Data for BP2-21 Quad Cities 2 Weld Irradiated in Capsule B B-42
Figure B-22 Charpy Energy Data for 406L44 Quad Cities 1 Weld Unirradiated B-44
Figure B-23 Charpy Energy Data for 406L44 Quad Cities 1 Weld Irradiated in Capsule A B-46
Figure B-24 Charpy Energy Data for 406L44 Quad Cities 1 Weld Irradiated in Capsule B B-48
Figure B-25 Charpy Energy Data for C3985-2 Hatch 1 Plate Unirradiated B-50
Figure B-26 Charpy Energy Data for C3985-2 Hatch 1 Plate Irradiated in Capsule C B-52
Figure B-27 Charpy Energy Data for C1079-1 Millstone 1 Plate Unirradiated B-54
Figure B-28 Charpy Energy Data for C1079-1 Millstone 1 Plate Irradiated in Capsule C B-56
Figure B-29 Charpy Energy Data for A0610-1 Quad Cities 1 Plate Unirradiated B-58
Figure B-30 Charpy Energy Data for A0610-1 Quad Cities 1 Plate Irradiated in Capsule C B-60
Figure B-31 Charpy Energy Data for A1195-1 HSST-02 Plate Unirradiated B-62
Figure B-32 Charpy Energy Data for A1195-1 HSST-02 Plate Irradiated in Capsule C B-64
Figure B-33 Charpy Energy Data for Cooper Weld 20291 Unirradiated B-66
Figure B-34 Charpy Energy Data for Cooper Weld 20291 Irradiated in Capsule C B-68
Figure B-35 Charpy Energy Data for AP2-BW B&W Linde 80 Weld Unirradiated B-70
Figure B-36 Charpy Energy Data for CP2-BW B&W Linde 80 Weld Irradiated in Capsule C B-72
Figure B-37 Charpy Energy Data for CP2-6 Humboldt Bay 3 Weld Unirradiated B-74
Figure B-38 Charpy Energy Data for CP2-6 Humboldt Bay 3 Weld Irradiated in Capsule C B-76
Figure B-39 Charpy Energy Data for 5P6756 River Bend Weld Unirradiated B-78
Figure B-40 Charpy Energy Data for 5P6756 River Bend Weld Irradiated in Capsule C B-80
Figure C-1 Schematic Representation of the SSP Capsule A Dosimetry Wire Layout Relative to the Charpy Test Specimens. C-17
Figure C-2 Schematic Representation of the SSP Capsule B Dosimetry Wire Layout Relative to the Charpy Test Specimens. C-18
Figure C-3 Schematic Representation of the SSP Capsule C Dosimetry Wire Layout Relative to the Charpy Test Specimens. C-19

LIST OF TABLES

Table 2-1 Thermal Monitors in SSP Capsule A 2-6
Table 2-2 SSP Capsules A, B, and C Charpy V-Notch Specimen Inventory 2-7
Table 2-3 Plate Materials Irradiated in SSP Capsules A, B, and C 2-8
Table 2-4 Weld Materials Irradiated in SSP Capsules A, B, and C 2-9
Table 2-5 Materials Irradiated in SSP (Cooper) Capsule A 2-10
Table 2-6 Materials Irradiated in SSP (Cooper) Capsule B 2-11
Table 2-7 Materials Irradiated in SSP (Cooper) Capsule C 2-12
Table 2-8 Baseline CVN Properties of SSP Capsule A Materials 2-13
Table 2-9 Baseline CVN Properties of SSP Capsule B Materials 2-14
Table 2-10 Baseline CVN Properties of SSP Capsule C Materials 2-15
Table 2-11 Results of Melt Wire Examination 2-17
Table 3-1 Summary of Material Compositions by Region for Cooper Nuclear Station 3-3
Table 3-2 Number of State-point Data Files for Cooper Nuclear Station Cycles 15-21 3-5
Table 3-3 Summary of Cooper Nuclear Station Core Loading Pattern for Cycles 15-21 3-6
Table 3-4 Sensitivity Analyses 3-12
Table 3-5 Energy Boundaries for the RAMA Neutron 47-Group Structure 3-14
Table 3-6 Row Positions of Response Functions in Tables 7001 and 7003 3-15
Table 3-7 Row Positions of Response Functions in Tables 7002 and 7004 3-16
Table 3-8 Comparison of Specific Activities for Cooper Nuclear Station SSP Capsule A Flux Wires 3-18
Table 3-9 Comparison of Specific Activities for Cooper Nuclear Station SSP Capsule A Dosimetry 3-19
Table 3-10 Comparison of Specific Activities for Cooper Nuclear Station SSP Capsule B Flux Wires 3-20
Table 3-11 Comparison of Specific Activities for Cooper Nuclear Station SSP Capsule B Dosimetry 3-21
Table 3-12 Comparison of Specific Activities for Cooper Nuclear Station SSP Capsule C Flux Wires 3-22
Table 3-13 Comparison of Specific Activities for Cooper Nuclear Station SSP Capsule C Dosimetry 3-23
Table 3-14 Best Estimate >1.0 MeV Neutron Fluence and Rated Power Flux in SSP Capsule A 3-24

Table 3-15 Best Estimate >1.0 MeV Neutron Fluence and Rated Power Flux in SSP Capsule B 3-24
Table 3-16 Best Estimate >1.0 MeV Neutron Fluence and Rated Power Flux in SSP Capsule C 3-25
Table 3-17 Best Estimate >0.1 MeV Neutron Fluence and Rated Power Flux in SSP Capsule A 3-25
Table 3-18 Best Estimate >0.1 MeV Neutron Fluence and Rated Power Flux in SSP Capsule B 3-26
Table 3-19 Best Estimate >0.1 MeV Neutron Fluence and Rated Power Flux in SSP Capsule C 3-26
Table 4-1 Drawing Showing the Charpy Test Specimen Geometry 4-3
Table 5-1 Effect of Irradiation (E>1.0 MeV) on the Notch Toughness Properties of Capsule A Materials 5-2
Table 5-2 Effect of Irradiation (E>1.0 MeV) on the Notch Toughness Properties of Capsule B Materials 5-3
Table 5-3 Effect of Irradiation (E>1.0 MeV) on the Notch Toughness Properties of Capsule C Materials 5-4
Table 5-4 Comparison of Actual Versus Predicted Embrittlement of SSP Capsule A Materials 5-6
Table 5-5 Comparison of Actual Versus Predicted Embrittlement of SSP Capsule B Materials 5-7
Table 5-6 Comparison of Actual Versus Predicted Embrittlement of SSP Capsule C Materials 5-8
Table 5-7 Percent Decrease in Upper Shelf Energy (USE) of SSP Capsule A Materials 5-9
Table 5-8 Percent Decrease in Upper Shelf Energy (USE) of SSP Capsule B Materials 5-10
Table 5-9 Percent Decrease in Upper Shelf Energy (USE) of SSP Capsule C Materials 5-11
Table A-1 Charpy V-Notch Results for Capsule A Plate A1224-1 ..... A-1
Table A-2 Charpy V-Notch Results for Capsule A Plate Heat C2331-2 ..... A-2
Table A-3 Charpy V-Notch Results for Capsule A Plate Heat P2130-2 ..... A-2
Table A-4 Charpy V-Notch Results for Capsule A Plate Heat C3278-2 ..... A-3
Table A-5 Charpy V-Notch Results for Capsule A Weld Heat 5P6214B A-3
Table A-6 Charpy V-Notch Results for Capsule A Weld Heat 34B009 ..... A-4
Table A-7 Charpy V-Notch Results for Capsule A Quad Cities 2 Electroslag Weld (Heat unknown) A-4
Table A-8 Charpy V-Notch Results for Capsule A Weld Heat 406L44 ..... A-5
Table A-9 Charpy V-Notch Results for Capsule B Plate Heat A1224-1 ..... A-5
Table A-10 Charpy V-Notch Results for Capsule B Plate Heat C2331-2 ..... A-6
Table A-11 Charpy V-Notch Results for Capsule B Plate Heat P2130-2 ..... A-6
Table A-12 Charpy V-Notch Results for Capsule B Plate Heat C3278-2 ..... A-7
Table A-13 Charpy V-Notch Results for Capsule B Weld Heat 5P6214B A-7
Table A-14 Charpy V-Notch Results for Capsule B Weld Heat 34B009 ..... A-8

Table A-15 Charpy V-Notch Results for Capsule B Quad Cities 2 Electroslag Weld (Heat unknown) A-8
Table A-16 Charpy V-Notch Results for Capsule B Weld Heat 406L44 ..... A-9
Table A-17 Charpy V-Notch Results for Capsule C Plate Heat C3985-2 ..... A-9
Table A-18 Charpy V-Notch Results for Capsule C Plate Heat C1079-1 ..... A-10
Table A-19 Charpy V-Notch Results for Capsule C Plate Heat A0610-1 ..... A-10
Table A-20 Charpy V-Notch Results for Capsule C Plate HSST-02 Heat A1195-1 ..... A-11
Table A-21 Charpy V-Notch Results for Capsule C Weld Heat 20291 ..... A-11
Table A-22 Charpy V-Notch Results for Capsule C B&W Linde 80 Weld (Heat unknown) A-12
Table A-23 Charpy V-Notch Results for Capsule C Humboldt Bay 3 Weld (Heat unknown) A-12
Table A-24 Charpy V-Notch Results for Capsule C Weld Heat 5P6756 ..... A-13
Table A-25 Charpy V-Notch Results for Unirradiated SSP Plate Heat A1224-1 ..... A-14
Table A-26 Charpy V-Notch Results for Unirradiated SSP Plate Heat C2331-2 ..... A-15
Table A-27 Charpy V-Notch Results for Unirradiated SSP Plate Heat P2130-2 ..... A-16
Table A-28 Charpy V-Notch Results for Unirradiated SSP Plate Heat C3278-2 ..... A-17
Table A-29 Charpy V-Notch Results for Unirradiated SSP Plate Heat C3985-2 ..... A-18
Table A-30 Charpy V-Notch Results for Unirradiated SSP Plate Heat C1079-1 ..... A-19
Table A-31 Charpy V-Notch Results for Unirradiated SSP Plate Heat A0610-1 ..... A-20
Table A-32 Charpy V-Notch Results for Unirradiated SSP Heat A1195-1 ..... A-21
Table A-33 Charpy V-Notch Results for Unirradiated SSP Weld 5P6214B A-22
Table A-34 Charpy V-Notch Results for Unirradiated SSP Weld 34B009 ..... A-23
Table A-35 Charpy V-Notch Results for Unirradiated SSP Quad Cities 2 Electroslag Weld (Heat unknown) A-24
Table A-36 Charpy V-Notch Results for Unirradiated SSP Weld 406L44 ..... A-25
Table A-37 Charpy V-Notch Results for Unirradiated SSP Weld 20291 ..... A-26
Table A-38 Charpy V-Notch Results for Unirradiated SSP B&W Linde 80 Weld (Heat unknown) A-27
Table A-39 Charpy V-Notch Results for Unirradiated SSP Humboldt Bay Weld (Heat unknown) A-28
Table A-40 Charpy V-Notch Results for Unirradiated SSP Weld 5P6756 ..... A-29
Table C-1 Cooper SSP Capsules A, B and C Wire Dosimeter Masses. C-5
Table C-2 Cooper SSP Capsules A, B and C Spectral Monitor Dosimeter Masses. C-7
Table C-3 GRSS Specifications. C-8
Table C-4 Counting Schedule for the Flux Wire Dosimeter Materials C-9
Table C-5 Counting Schedule for the Spectral Monitor Dosimeter Materials C-11
Table C-6 Neutron-Induced Reactions of Interest. C-12
Table C-7 Results of the Radiometric Analysis for the Flux Wires C-13
Table C-8 Results of the Radiometric Analysis for the Spectral Monitors C-15

1
INTRODUCTION

Test coupons of reactor vessel ferritic beltline materials are irradiated in reactor surveillance capsules to facilitate evaluation of vessel fracture toughness in vessel integrity evaluations. The key values that characterize fracture toughness are the reference temperature of nil-ductility transition (RT_{NDT}) and the upper shelf energy (USE). These are defined in 10CFR50 Appendix G [1] and in Appendix G of the ASME Boiler and Pressure Vessel Code, Section XI [2]. Appendix H of 10CFR50 [1] and ASTM E185-82 [3] establish the methods to be used for testing of surveillance capsule materials.

In the late 1980's the BWR Owners' Group (BWROG) initiated the Supplemental Surveillance Program (SSP) [4] to obtain BWR surveillance data to supplement the individual plant surveillance programs. Nine (9) capsules containing test specimens were placed in two host reactors as part of the SSP. Three capsules (designated A, B, and C) were placed into the Cooper reactor, and the remaining six capsules (D through I) were placed into the Oyster Creek reactor.

In the late 1990's the BWR Vessel and Internal Project (BWRVIP) initiated the BWRVIP Integrated Surveillance Program (ISP) [5]. The SSP capsules were included in the ISP because the SSP materials represent a wide range of BWR beltline materials and their baseline properties were well-characterized. The BWRVIP assumed responsibility for testing and evaluation of the SSP capsules.

This report addresses the final set of SSP capsules (Capsules A, B, and C) to be removed and tested. The three surveillance capsules were installed within the Cooper Nuclear Station (CNS) in November, 1991 and removed in March, 2003. The surveillance capsules contained flux wires for neutron flux monitoring, Charpy V-notch impact test specimens fabricated using materials from a variety of sources, and thermal monitors. The capsules were shipped to MPM Technologies, Inc., for testing. Evaluation of the fluence environment was conducted by TransWare Enterprises, Inc. Final evaluation of the Charpy test data and irradiated material properties and compilation of this report were performed by ATI Consulting. The capsule materials have been tested per ASTM E185-82, and the information and the associated evaluations provided in this report have been performed in accordance with the requirements of 10CFR50 Appendix B.

This report compares the irradiated material properties to the unirradiated properties. The observed embrittlement (as characterized by ΔT_{30}) is compared to that predicted by U.S. Nuclear Regulatory Commission (USNRC) Regulatory Guide 1.99, Rev. 2 [6]. Eleven (11) of the sixteen (16) materials in the three capsules are used or tracked in the BWRVIP ISP. For those materials, other BWRVIP ISP reports will integrate these shift results with other surveillance capsule results for a broader characterization of embrittlement behavior.

1.1 Implementation Requirements

The results documented in this report will be utilized by the BWRVIP ISP and by individual utilities to demonstrate compliance with 10CFR50, Appendix H, Reactor Vessel Material Surveillance Program Requirements. Therefore, the implementation requirements of 10CFR50, Appendix H govern and the implementation requirements of Nuclear Energy Institute (NEI) 03-08, Guideline for the Management of Materials Issues, are not applicable.

2
MATERIALS AND TEST SPECIMEN DESCRIPTION

SSP Capsules A, B, and C were designed and built by GE Nuclear Energy [4]. They contained flux wires for neutron flux monitoring, Charpy V-notch (CVN) impact test specimens fabricated using materials from a variety of sources, and thermal monitors. These monitors and specimens are described in the following sections. Schematics from [4] showing the general layout of SSP Capsules A, B, and C are provided in Figures 2-1, 2-2, and 2-3, respectively. The three capsules were contained in a single capsule holder mounted to the inside wall of the Cooper reactor vessel as shown in Figure 2-4.

2.1 Dosimeters

Each capsule contained a variety of neutron dosimeter materials. Since the surveillance capsules were up to about 20 inches (0.51 m) in axial height, full length copper and iron flux wires were placed in the capsules to provide dosimetry data for each set of 10 Charpy specimens (which were stacked axially). By cutting each wire to lengths corresponding to the locations of each specimen set and analyzing separately, it was possible to determine a fluence for each Charpy specimen set.

All three capsules also contained an additional set of wires and foils placed in gadolinium capsules which are intended for neutron energy spectrum measurements. The spectral dosimetry capsules were irradiated near the bottom of each capsule. The gadolinium dosimetry cylinders in each capsule were identical and included: iron wires (4); copper wire (1); nickel wire (1); niobium wire (1); titanium wire (1); aluminum-cobalt wire (1); and silver foil (1). As designed by GE, the four Fe wires were positioned at 90° intervals around the circumference of the gadolinium capsule for flux gradient determination.

A detailed discussion of the capsule dosimetry, including schematics showing dosimeter wire layout relative to the Charpy test specimens and the results of radiometric analysis, is provided in Appendix C of this report.

2.2 Thermal Monitors

Five thermal monitors were included in Capsule A to provide data needed to bound the peak irradiation temperature. As shown in Figure 2-5, the thermal monitors consist of melt wires which are housed in quartz tubes. The melt wire material is a eutectic material which is designed to melt within 4°F (2.2°C) of a specified temperature. The water temperature in the annulus region of a BWR depends on the feedwater temperature, but typically ranges between 525°F (274°C) and 535°F (279°C). Accordingly, GE designed the melt wire temperatures to cover this

range [4], and the target melting temperatures are summarized in Table 2-1. The quartz tube lengths are used to identify the melt wire materials.

Content Deleted -
EPRI Proprietary Information

Figure 2-1
Cooper SSP Capsule A

Content Deleted -
EPRI Proprietary Information

Figure 2-2
Cooper SSP Capsule B

Content Deleted -
EPRI Proprietary Information

Figure 2-3
Cooper SSP Capsule C

Content Deleted -
EPRI Proprietary Information

Figure 2-4
Cooper Nuclear Station SSP Capsule Holder

Content Deleted -
EPRI Proprietary Information

Figure 2-5
Schematic Representation of Thermal Monitor

Table 2-1
Thermal Monitors in SSP Capsule A

Melt Wire Composition (Weight %)	Target Melting Temperature[1] °F (°C)	Quartz Tube Length inches (cm)
73.7 Pb, 25 Sn, 1.3 Sb	504 (262)	1.0 (2.54)
81 Pb, 19 In	518 (270)	1.25 (3.18)
80 Au, 20 Sn	536 (280)	1.5 (3.81)
90 Pb, 5 Ag, 5 Sn	558 (292)	1.75 (4.45)
97.5 Pb, 2.5 Ag	580 (304)	2.0 (5.08)

[1]Melt wires are designed to melt within 4°F (2.2°C) of the specified temperatures.

2.3 Charpy V-Notch Specimens

The Charpy V-notch loading inventory, chemical compositions, material descriptions, and unirradiated (baseline) mechanical properties of the materials irradiated in SSP Capsules A, B, and C are summarized below.

2.3.1 Capsule Loading Inventory

The capsule loading inventory is provided in Table 2-2. Each capsule contained a set of ten (10) Charpy V-notch specimens for eight (8) materials, for a total of 80 CVN specimens in each capsule. The SSP capsules contained no tensile specimens and no CVN specimens for heat-affected zone (HAZ) materials.

Four (4) of the eight materials in each capsule were plate materials and four (4) were weld materials. The material heats loaded into Capsules A and B were identical; a different set of materials was loaded into Capsule C. A total of eight (8) plate materials and eight (8) weld materials were irradiated in SSP Capsules A, B, and C.

Table 2-2
SSP Capsules A, B, and C Charpy V-Notch Specimen Inventory

Content Deleted -
EPRI Proprietary Information

2.3.2 Material Description

SSP capsules A, B, and C contained archive materials from BWR surveillance programs, HSST-02 standard material, and a B&W Linde 80 weld from B&W. All specimens were machined by GE from archive plant material, with the following exceptions: The Cooper weld 20291 specimens were archive specimens fabricated at the same time as the standard Cooper surveillance weld specimens; the B&W Linde 80 weld specimens were fabricated by GE from a block provided by B&W; and the HSST-02 plate specimens were also fabricated by GE from a full thickness block provided by Oak Ridge National Laboratory [5].

Tables 2-3 and 2-4 contain information about the specimens in SSP (Cooper) Capsules A, B, and C including fabricator, and copper and nickel content. Table 2-3 presents plate materials and Table 2-4 describes the weld materials.

Table 2-3
Plate Materials Irradiated in SSP Capsules A, B, and C

Content Deleted -
EPRI Proprietary Information

Table 2-4
Weld Materials Irradiated in SSP Capsules A, B, and C

Content Deleted -
EPRI Proprietary Information

2.3.3 Chemical Composition

Tables 2-5, 2-6, and 2-7 provide the best estimate chemistry composition of the surveillance materials in SSP Capsules A, B, and C, respectively.

Eleven of the sixteen materials in SSP Capsules A, B, and C are used in the BWRVIP ISP as Representative Surveillance Materials or are tracked by the ISP because they are heats used in the beltlines of BWR plants. For each of those eleven materials, a calculation of the best estimate chemistry is documented in BWRVIP-135 [7], ISP Data Source Book and Plant Evaluations. Each calculation in BWRVIP-135 considered all valid chemistry data for the surveillance material, including GE measurements on the SSP specimens [8] and chemistry measurements by the parent surveillance program from which the archive specimens came to the SSP. Therefore, BWRVIP-135 is used as the source of the best estimate chemistry for those eleven materials. For the other five materials, the best estimate was determined from chemistry measurements conducted by GE on the materials at the time of capsule assembly [8].

Table 2-5
Materials Irradiated in SSP (Cooper) Capsule A

Content Deleted -
EPRI Proprietary Information

Table 2-6
Materials Irradiated in SSP (Cooper) Capsule B

Content Deleted -
EPRI Proprietary Information

Table 2-7
Materials Irradiated in SSP (Cooper) Capsule C

Content Deleted -
EPRI Proprietary Information

2.3.3 CVN Baseline Properties

Tables 2-8, 2-9 and 2-10 provide a summary of the baseline (unirradiated) Charpy V-notch properties of the SSP Capsules A, B, and C materials, respectively. In these tables and throughout this report, T_{30} is the 30 ft-lb (41 J) transition temperature; T_{50} is the 50 ft-lb (68 J) transition temperature; T_{35mil} is the 35 mil (0.89 mm) lateral expansion temperature; and USE is the average energy absorption at full shear fracture appearance.

Content Deleted -
EPRI Proprietary Information

Table 2-8
Baseline CVN Properties of SSP Capsule A Materials

Content Deleted -
EPRI Proprietary Information

Table 2-9
Baseline CVN Properties of SSP Capsule B Materials

Content Deleted -
EPRI Proprietary Information

Table 2-10
Baseline CVN Properties of SSP Capsule C Materials

Content Deleted -
EPRI Proprietary Information

2.4 Capsule Opening

The surveillance capsules were opened in August, 2005. The outside of the capsules had identification markings which were difficult to read. The capsule identification was determined from the marked Charpy bars inside the capsules. As expected, a total of 80 Charpy V-notch specimens were recovered from each capsule with the identifications listed in Table 2-2.

2.4.1 Condition of Dosimeters

Particular attention was paid to the specimen and dosimeter wire locations during disassembly of the capsules. As shown in Figures 2-6 through 2-9, the Fe and Cu dosimeter wires which extended over the axial length of the capsules were not in the Charpy notches over significant axial distances in all three capsules. GE intended that the dosimetry wires should be irradiated in the Charpy notches. A possible explanation is that the wires were dislodged by the post-irradiation handling. However, the only visible damage on the outside of the capsules was bent U-hooks at the top of the capsules. This damage could have happened when the capsules were

removed from service. There were no indications that the capsules had been dropped or otherwise impacted.

Further, several observations point to the conclusion that the wires were not in the Charpy notches during the entire irradiation:

- the capsule outer wrapper is so tight after exposure to the high pressure of the primary system that it is not possible for the wires to move very far
- the external surface of the capsule wrappers (ex, see Figure 2-6) have visible impressions of the wire and have contoured around the wires due to the coolant pressure
- there is a linear mark on the surface of the Charpy specimens showing where the wires were positioned during irradiation
- the wires were not "locked in" at the bottom of the capsules which allowed them to come out of the Charpy notches

These observations point to the capsules being irradiated with the wires out of the notches. It is possible that the wires moved before the initial pressurization in reactor water and then were held in place out of the Charpy notches between the outer stainless steel wrapper and the specimens. It can be difficult to get the stainless steel wrapper tight initially during fabrication. The wires were configured so that they were locked into position at the top of the capsules but not at the bottom. Not locking the wires in at the bottom of the capsule is a serious design deficiency which most likely led to the wires being irradiated out of the Charpy notches over most of the length of the capsules. In cases where there is a large flux variation with azimuthal angle, it is necessary to account for the wire position in the capsule to obtain good agreement between calculation and measurement.

As shown in Figures 2-6 through 2-8, the capsules were opened by removing the top face of the wrapper to reveal the specimens and dosimetry. As discussed in [4], the Charpy specimens were arranged in two parallel columns with four groups of ten specimens in each column. Therefore, the Fe and Cu wires were cut into axial segments which span the group of ten Charpy bars to enable measured fluence determination for each set of Charpy specimens. In addition to the Fe and Cu wire dosimetry, the spectral dosimetry for each of the capsules was successfully recovered along with the thermal monitors from Capsule A.

2.4.2 Condition of Thermal Monitors

Content Deleted -
EPRI Proprietary Information

Table 2-11
Results of Melt Wire Examination

Content Deleted -
EPRI Proprietary Information

Content Deleted -
EPRI Proprietary Information

Figure 2-6
Photograph of CNS Capsule A Wrapper Showing Indentations which Indicate that the Capsule was Irradiated with the Dosimetry Wires out of the Charpy Notches.

Content Deleted -
EPRI Proprietary Information

Figure 2-7
Photograph of CNS Capsule A Showing Fe and Cu Wires Out of the Charpy Notches.
(Capsule U-Hook is at Top of Photograph)

Content Deleted -
EPRI Proprietary Information

Figure 2-8
Photograph of CNS Capsule B Showing Fe and Cu Wires Out of the Charpy Notches.
(Capsule U-Hook is at Top of Photograph)

Content Deleted -
EPRI Proprietary Information

Figure 2-9
Photograph of CNS Capsule C Showing Fe and Cu Wires Out of the Charpy Notches.
(Capsule U-Hook is at Top of Photograph)

3
NEUTRON FLUENCE CALCULATION

3.1 Description of the Reactor System

This section describes the Cooper Nuclear Station (CNS) design inputs used in the surveillance capsule activation and fluence evaluation performed per the guidance of Regulatory Guide 1.190 [12]. The basic design inputs include component mechanical designs, material compositions, and reactor operating history. Mechanical design drawings and structural material data were provided by Nebraska Public Power District and were used to build the Cooper Nuclear Station RAMA geometry model [13]. Detailed operating history data was provided for this project by Nebraska Public Power District [14] for cycles 15 through 21.

3.1.1 Reactor System Mechanical Design Inputs

The CNS employs a boiling water reactor (BWR) nuclear steam supply system. The reactor is a General Electric BWR/4 class reactor and the reactor core consists of 548 fuel assemblies with a rated thermal power of 2381 MWt.

The CNS is modeled with the RAMA Fluence Methodology [15-19]. The Methodology employs a three-dimensional modeling technique to describe the reactor geometry for the neutron transport calculations. Detailed mechanical design information is used in order to build an accurate three-dimensional RAMA computer model of the reactor system. A summary of the important design inputs is presented in this subsection.

Figure 3-1 illustrates the basic planar geometry configuration of the reactor at the axial elevation corresponding to the core mid-plane elevation. All radial regions comprising the fluence model are illustrated. Beginning at the center of the reactor and projecting outwards, the regions include: the core region, including control rod locations and fuel assembly locations (fuel locations are shown only for the northeast quadrant); core reflector region (bypass water); central shroud wall; downcomer water region including the jet pumps; reactor pressure vessel (RPV) wall; mirror insulation; biological shield (concrete wall); and cavity regions between the RPV and biological shield. Also shown are the azimuthal positions of the surveillance capsules in the downcomer region at 30°, 120°, and 300°. The surveillance capsules are positioned radially near the inner surface of the RPV wall. The azimuthal positions of the jet pump assemblies are illustrated as well at 30°, 60°, 90°, 120°, 150°, 210°, 240°, 270°, 300°, and 330°.

The specimen locations in SSP surveillance capsules A, B, and C, and the capsule holder design showing the positioning of the A, B, and C capsules within the holder (e.g., Figure 2-4), were described in the previous chapter.

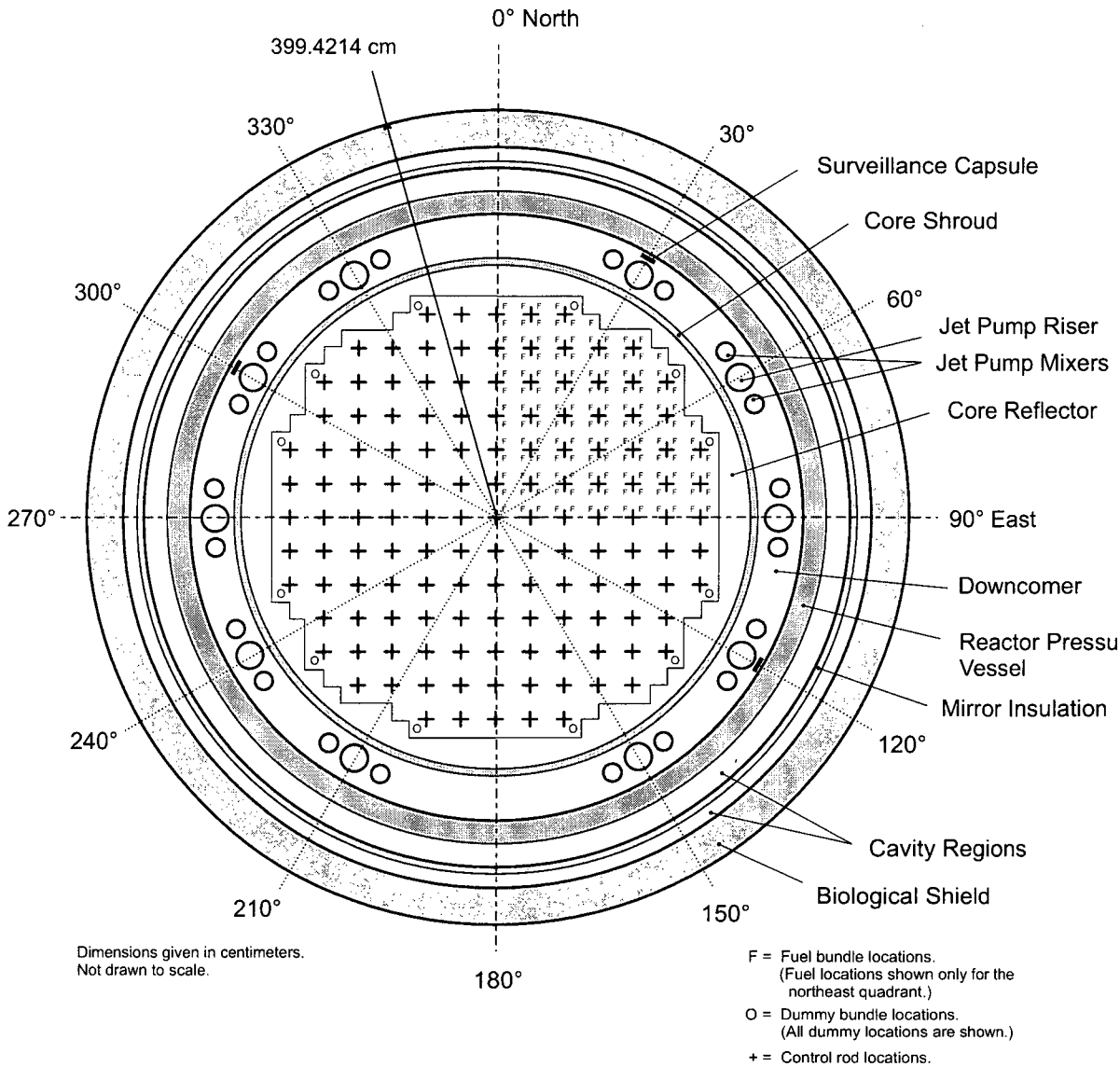

Figure 3-1
Planar View of the Cooper Nuclear Station Reactor

3.1.2 Reactor System Material Compositions

Each region of the reactor is comprised of materials that include reactor fuel, steel, water, insulation, concrete, and air. Accurate material information is essential for the fluence evaluation as the material compositions determine the scattering and absorption of neutrons throughout the reactor system and, thus, affect the determination of neutron fluence in the reactor components.

Table 3-1 provides a summary of the material compositions in the various components and regions of the CNS. The attributes for the steel, insulation, concrete, and air compositions (i.e., material densities and isotopic concentrations) are assumed to remain constant for the operating life of the reactor. The attributes for the ex-core water compositions will vary with the operation of the reactor, but are generally represented at nominal hot operating conditions and are assumed to be constant throughout an operating cycle.

Table 3-1
Summary of Material Compositions by Region for Cooper Nuclear Station

Region	Material Composition
Reactor Core	^{235}U, ^{238}U, ^{239}Pu, ^{240}Pu, ^{241}Pu, ^{242}Pu, O_{fuel}, Zr, Water
Core Reflector	Water
Fuel Support Piece	Stainless Steel
Fuel Assembly Lower Tie Plate	Stainless Steel, Zircaloy, Inconel
Fuel Assembly Upper Tie Plate	Stainless Steel, Zircaloy, Inconel
Top Guide	Stainless Steel
Shroud	Stainless Steel
Jet Pump Riser and Mixer Flow Area	Water
Jet Pump Riser and Mixer Metal	Stainless Steel
Downcomer Region	Water
Surveillance Capsule	Carbon Steel
Reactor Pressure Vessel Clad	Stainless Steel
Reactor Pressure Vessel Wall	Carbon Steel
Cavity Regions	Air (Oxygen)
Insulation	Stainless Steel
Biological Shield Clad	Carbon Steel
Biological Shield	Reinforced Concrete

The attributes of the fuel compositions in the reactor core region change continuously during an operating cycle due to changes in power level, fuel burnup, control rod movements, and changing moderator density levels (voids). Because of the dynamics of the fuel attributes with reactor operation, one to several data sets describing the operating state of the reactor core are used for each operating cycle. The number of data sets used in this analysis is presented in Section 3.1.3.2.

3.1.3 Reactor Operating Data Inputs

An accurate evaluation of fluence in the CNS requires an accurate accounting of the reactor operating history. The primary reactor operating parameters that affect neutron fluence evaluations for BWR's include the reactor power level, core power distribution, core void fraction distribution (or equivalently, water density distribution), and fuel material distribution. These items are described in the following subsections.

3.1.3.1 Power History Data

The reactor power history used in the CNS surveillance capsule fluence evaluation was obtained from daily power history edits provided by Nebraska Public Power District for operating cycles 15 through 21 [14]. The daily power values represent step changes in power on a daily basis and are assumed to be representative of the power over the entire day. The surveillance capsule fluence evaluation for the CNS considers the complete daily operating history of the reactor from cycles 15 through 21. Also accounted for in the analysis are the shutdown periods. The shutdowns were primarily due to the refueling outages between cycles. Table 3-2 provides the effective full power years of power generation at the end of each cycle in this capsule fluence evaluation.

3.1.3.2 Reactor State Point Data

CNS operating data for the capsule fluence evaluation was provided as state point data files by Nebraska Public Power District [14]. The state point files provide a best-available representation of the operating conditions of the unit over the operating lifetime of the reactor. The data files include three-dimensional data arrays that describe the fuel materials, moderator densities, and relative power distribution in the core.

A total of 79 state point data files were used to represent operating cycles 15 through 21 of the CNS. Table 3-2 shows the number of state point data files for each cycle used in this capsule fluence evaluation. A separate neutron transport calculation was performed for each state point. The calculated neutron flux for each state point was combined with the appropriate power history data described in Section 3.1.3.1 in order to predict the neutron fluence in the surveillance capsules.

Table 3-2
Number of State-point Data Files for Cooper Nuclear Station Cycles 15-21

Content Deleted -
EPRI Proprietary Information

3.1.3.3 Core Loading Pattern

It is common in BWRs that more than one fuel assembly design will be loaded in the reactor core in any given operating cycle. For fluence evaluations, it is important to account for the fuel assembly designs that are loaded in the core in order to accurately represent the neutron source distribution at the core boundaries (i.e., peripheral fuel locations, the top fuel nodes, and the bottom fuel nodes).

Three different fuel assembly designs are used in the CNS during cycles 15 through 21. Table 3-3 provides a summary of the fuel designs loaded in the reactor core for these operating cycles. The cycle core loading patterns provided by Nebraska Public Power District are used to identify the fuel assembly designs in each cycle and their location in the core loading pattern. For each cycle, appropriate fuel assembly models are used to build the reactor core region of the RAMA fluence model for the CNS.

Table 3-3
Summary of Cooper Nuclear Station Core Loading Pattern for Cycles 15-21

Content Deleted -
EPRI Proprietary Information

3.2 Calculation Methodology

The Cooper Nuclear Station fluence evaluations were performed using the RAMA Fluence Methodology software package. The Methodology and the application of the Methodology to the Cooper Nuclear Station reactor are described in this section.

3.2.1 Description of the RAMA Fluence Methodology

The RAMA Fluence Methodology software package is a system of codes that is used to perform fluence evaluations in light water reactor components. The significance of the Methodology is the integration of a three-dimensional arbitrary geometry modeling technique with a deterministic transport method to provide a flexible and accurate platform for determining neutron fluence in light water reactor systems. The Methodology is complemented with model building codes to prepare the three-dimensional models for the transport calculation and a post-processing code to calculate fluence from the neutron flux calculated by the transport code.

The primary inputs for the RAMA Fluence Methodology are mechanical design parameters and reactor operating history data. The mechanical design inputs are obtained from reactor design drawings (or vendor drawings) of the plant. The CNS operating history data is obtained from reactor core simulation calculations, system heat balance calculations, and daily operating logs that describe the operating conditions of the reactor.

The primary outputs from the RAMA Fluence Methodology calculations are neutron flux, neutron fluence, and uncertainty determinations. The RAMA transport code calculates the neutron flux distributions that are used in the determination of neutron fluence. Several transport calculations are typically performed over the operating life of the reactor in order to calculate neutron flux distributions that accurately characterize the operating history of the reactor. The

post-processing code (RAFTER) is then used to calculate component fluence and nuclide activations using the neutron flux solutions from the transport calculations and daily operating history data for the plant. The fluence calculated by RAFTER may then be adjusted in accordance with the calculational bias to determine the best estimate fluence and uncertainty in accordance with the intent of U. S. Nuclear Regulatory Guide 1.190.

3.2.2 The RAMA Geometry Model for Cooper Nuclear Station

Figure 3-2 illustrates the planar configuration of the CNS model at an axial elevation near the core mid-plane of the reactor pressure vessel. In the radial dimension the model extends from the center of the RPV to the outside surface of the biological shield (399.4214 cm). Nine radial regions are defined in the CNS model: the core region (comprised of interior and peripheral fuel assemblies), core reflector, shroud, downcomer region with jet pumps, pressure vessel, mirror insulation, biological shield, and inner and outer cavity regions. The RPV has cladding on the wall inner surface. The biological shield has cladding on the inner and outer surfaces.

Figure 3-2 shows that the reactor core region is modeled with rectangular geometry to preserve the shape of the core region. The core region is characterized with two layers: the interior fuel assemblies and the peripheral fuel assemblies. The peripheral fuel assemblies are the primary contributors to the neutron source in the fluence calculation and are modeled to preserve the pin-wise source contribution at the core-core reflector interface.

Each of the components and regions that extend outward from the core region are modeled in their correct geometrical form. The core shroud, downcomer, RPV wall, mirror insulation, biological shield wall, and cavity regions are correctly modeled as cylindrical parts. The jet pump assembly design is properly modeled using cylindrical pipe elements for the jet pump riser and mixer pipes. The riser pipe is correctly situated between the mixer pipes. The surveillance capsule, which is rectangular in design, is modeled as an arc element in the geometry and is correctly positioned near the inner surface of the RPV wall. This model is an acceptable approximation since the capsule is a sufficient distance from the core center that the arc element closely approximates the shape of a rectangular element. Downcomer water surrounds the capsule on all sides.

The jet pumps are shown as modeled at azimuth 30° in the downcomer region. When symmetry is applied to the model, the jet pump assemblies that are positioned azimuthally at 30°, 60°, 120°, 150°, 210°, 240°, 300°, and 330° are represented by the model. Due to model symmetry restrictions, the jet pumps at the 90° and 270° azimuths are not represented. This is a conservative approximation for RPV fluence calculations and is assumed to be applicable to other components. The surveillance capsules are shown as modeled at azimuth 30°. When symmetry is applied to the model, this location represents each of the surveillance capsules loaded at 30°, 120°, and 300° (see Figure 3-1).

Content Deleted -
EPRI Proprietary Information

Figure 3-2
Planar View of the Cooper Nuclear Station RAMA Model

As shown in Figure 3-1, the CNS geometry is quadrant symmetric, both in the core region and in the ex-core geometry. The quadrant core symmetry results from the presence of 12 dummy bundles, eight of which are located in octant symmetric locations, and four of which are located in quadrant symmetric locations. The ex-core symmetry results from the presence of ten jet pump assemblies that are located in quadrant-symmetric locations. For computational reasons, the RAMA model of the CNS core and ex-core geometry assumes octant symmetry. In the azimuthal dimension the model spans from 0° to 45° where the 0° azimuth corresponds to the north compass direction that is specified in the reactor design drawings. The selection of this octant is appropriate because the SSP capsules are located at the 30° azimuth.

Figure 3-3 provides an illustration of the axial configuration of the CNS RAMA model for three significant components: a fuel column, the core shroud, and the reactor pressure vessel. Also shown in the figure are the relative axial positioning of the jet pumps, surveillance capsules, and core spray sparger pipes in the reactor model. The axial planes are divided into several groups representing particular component regions of the model as follows: the core region, the top guide, the shroud head flange, the core spray spargers, the fuel support piece, core support plate, and core inlet region. Sub-planar meshing is used in the model, as needed, to properly represent the positioning of reactor components, such as the jet pump rams head and surveillance capsules. The model consists of thousands of mesh regions. In the axial direction, the CNS fluence model spans from below the jet pump riser inlet to above the core shroud head flange for a total of 631.3488 cm (20.7 feet) in length.

There are several key features of the RAMA code system that allow the CNS design to be accurately represented for component fluence evaluations; key features of the model include:

- Rectangular and cylindrical bodies are mixed in the model in order to provide an accurate geometrical representation of the components and regions in the reactor.
- The core geometry is modeled using rectangular bodies to represent the fuel assemblies in the reactor core region.
- Cylindrical bodies are used to represent the components and regions that extend outward from the core region.
- A combination of rectangular and cylindrical bodies is used to describe the transition parts that are required to interface the rectangular core region to the cylindrical outer core regions.
- The top guide is appropriately modeled by including a representation of the vertical fuel assembly parts and top guide plates. The upper fuel assembly parts that extend into the top guide region are modeled in three axial segments: the fuel rod plenum, fuel rod upper end plugs, and fuel assembly upper tie plate.
- The fuel support piece, core support plate, and core inlet regions appropriately include a representation of the cruciform control rod below the core region. The lower fuel assembly parts include representations for the fuel rod lower end plugs, lower tie plate, and nose piece.
- The surveillance capsules are accurately represented in the downcomer region at the correct azimuthal, radial, and axial locations.

Content Deleted -
EPRI Proprietary Information

Figure 3-3
Axial View of the Cooper Nuclear Station RAMA Model

3.2.3 RAMA Calculation Parameters

The RAMA transport code uses a three-dimensional deterministic transport method to calculate neutron flux distributions in reactor problems. The transport method is based on a numerical integration technique that uses ray-tracing to form the integration paths through the problem geometry. The integration paths for the rays are determined using four parameters. The distance between parallel rays in the planar dimension is specified as 1.00 cm. The distance between parallel rays in the axial dimension is specified as 5.00 cm. The depth that a ray penetrates a reflective boundary is specified as 10 mean free paths. In accordance with the guidelines provided in [12], the angular quadrature for determining ray trajectories is specified as S8, which provides an acceptable compromise between computational accuracy and performance.

The RAMA transport calculation also uses information from the RAMA nuclear data library to determine the scope of the flux calculation. This information includes the Legendre order of expansion that is used in the treatment of anisotropy of the problem. By default, the RAMA transport calculation uses the maximum order of expansion that is available for each nuclide in the RAMA nuclear data library (i.e., through P_5 scattering for actinide and zirconium nuclides and through P_7 scattering for all other nuclides in the model).

The neutron flux is calculated using an iterative technique to obtain a converged solution for the problem. The convergence criterion used in the evaluation is 0.01 which provides an asymptotic solution.

The impact of these calculation parameter selections on the RAMA capsule fluence evaluation for Cooper Nuclear Station is presented in Section 3.2.6.

3.2.4 RAMA Neutron Source Calculation

The neutron source for the RAMA transport calculation is calculated using the input relative power density factors for the different fuel regions and data from the RAMA nuclear data library.

The core neutron source was determined using the cycle-specific three-dimensional burnup distributions. The source distributions account for the radial power gradient in the fuel assemblies loaded near the core boundary by modeling the pin-wise source distributions in the outer row of fuel assemblies.

3.2.5 RAMA Fission Spectra

RAMA calculates a weighted fission spectrum, based on the relative contributions of the fuel isotopes, that is used in the transport calculation. The fission spectra for ^{235}U, ^{238}U, ^{239}Pu, ^{240}Pu, ^{241}Pu, and ^{242}Pu that are used in the RAMA transport calculations were taken directly from the latest release of the BUGLE-96 data library.

3.2.6 Parametric Sensitivity Analyses

Several sensitivity analyses were performed to evaluate the stability and accuracy of the RAMA transport calculation for the Cooper Nuclear Station model. Several parameters were evaluated including mesh size and the integration parameters discussed earlier. A summary of the analyses is presented in Table 3-4. As provided for in [12], two-dimensional models consisting of the detailed planar representation at the core mid-plane, typical of the model shown in Figure 3-2, are used to evaluate the sensitivities for those parameters that are insensitive to axial variations. Those parameters that are sensitive to axial variations are evaluated using detailed three-dimensional models typical of the model.

Table 3-4
Sensitivity Analyses

Content Deleted -
EPRI Proprietary Information

3.3 RAMA Nuclear Data Library

The nuclear cross section library is an essential element in neutron fluence evaluations. The accuracy of the cross section data is one of the primary factors that affect the accuracy of the neutron fluence prediction in reactor components. The RAMA nuclear data library is based upon the BUGLE-96 library [20] which has been developed exclusively from ENDF/B-VI nuclear data by Oak Ridge National Laboratories.

3.3.1 Nuclear Cross Sections

The RAMA nuclear data library consists of 47 neutron energy groups that span an energy range of 0.1 eV to 17.332 MeV. The group structure is especially well-suited to applications requiring accurate determination of neutron flux with energy >1.0 MeV. This is of primary importance in the evaluation of irradiation damage to reactor components. The RAMA nuclear data library also includes energy group upscattering in the lower (thermal) energy range of <5.04 eV. This significantly improves the prediction of thermal flux. Table 3-5 shows the group structure for the 47 neutron groups in the RAMA nuclear data library. The RAMA nuclear data library contains an extensive set of nuclide cross sections that are pre-shielded and spectrally collapsed using light water reactor flux spectra. The library incorporates improved resonance treatments for steel nuclides that are based on ENDF-B/VI. The resonance treatments are of particular importance in reactor system component fluence evaluations. Except for oxygen in the reactor cavity regions, surveillance capsule evaluations use appropriately pre-shielded and spectrally collapsed cross section data.

The RAMA nuclear data library has been especially developed for the solution of ex-core neutron transport calculations that must account for anisotropic scattering effects. Lighter nuclides contain scattering data for up to P_7 Legendre scattering expansion, while the heavier nuclides contain data for up to P_5 scattering.

Table 3-5
Energy Boundaries for the RAMA Neutron 47-Group Structure

Content Deleted -
EPRI Proprietary Information

3.3.2 Activation Response Functions

Response functions are used to calculate nuclear reactions and other integral parameters (e.g., integrated fluxes over various energy ranges) of interest in ex-core calculations. Tables 3-6 and 3-7 list the activation response functions included in the RAMA nuclear data library.

The response function tables are identified in the RAMA nuclear data library with the nuclide identifiers 7001, 7002, 7003, and 7004. Response tables 7001 (Part A) and 7002 (Part B) contain response functions which have a flat weighting corresponding to the in-vessel surveillance capsule location. Response tables 7003 (Part A) and 7004 (Part B) contain response functions which have a weighting corresponding to the 1/4T location in the pressure vessel.

Table 3-6
Row Positions of Response Functions in Tables 7001 and 7003

Content Deleted -
EPRI Proprietary Information

Table 3-7
Row Positions of Response Functions in Tables 7002 and 7004

Content Deleted -
EPRI Proprietary Information

3.4 Surveillance Capsule Activation Results

This section contains the results from the CNS SSP capsules A, B, and C activation analysis. The predicted activations (i.e., specific activities) generated by the RAMA Fluence Methodology were compared to the activation measurements for the capsule flux wires (see Appendix C) and are presented here. CNS SSP capsules A, B, and C were positioned in the reactor at azimuth 30° and were removed at the end of cycle 21 after being irradiated for six cycles for a total of 8.5 effective full power years (EFPY).

Copper and iron flux wires were irradiated in the CNS SSP capsules A, B, and C. Activation measurements were performed following irradiation for the following reactions (see Appendix C): $^{63}Cu(n,\alpha)^{60}Co$ and $^{54}Fe(n,p)^{54}Mn$. Additional activation samples were present in gadolinium dosimetry containers in each capsule. These additional samples included iron and copper wires, as well as wire and foil samples for the following activation reactions: $^{58}Ni(n,p)^{58}Co$, $^{46}Ti(n,p)^{46}Sc$, $^{93}Nb(n,\gamma)^{94}Nb$, $^{59}Co(n,\gamma)^{60}Co$, and $^{109}Ag(n,\gamma)^{110}Ag$. However, the activation levels for the nickel and titanium reactions were too low due to extensive decay of the samples to provide reliable measurement results and are provided for information only in Appendix C. The niobium reaction is not included in the BUGLE-96 based RAMA nuclear data library, so no comparisons are provided for this reaction. Both the cobalt and silver reactions are predominately the result of

absorptions in the thermal energy range. The thermal spectrum is attenuated by the gadolinium dosimetry container, however, the RAMA nuclear data library does not include gadolinium so that appropriate attenuation of the thermal spectrum can not be represented in the RAMA evaluation. Accordingly, comparison results are not provided for these reactions in the RAMA activation evaluation.

It was also observed that the copper and iron flux wires had become displaced from their customary position along the V-groove of the Charpy sample specimens at some point during irradiation. As a result, the specific location of the individual wires within the capsules is not known so the RAMA calculation was performed assuming that the wires were located at the lateral center of the capsules. The potential impact of this assumption was evaluated by comparing the predicted activity at various azimuthal positions to the predicted value from the lateral center of the capsules. For the most sensitive capsule (capsule B), the maximum azimuthal value is about 3% higher than the value at the center of the capsule, and the minimum azimutal value is about 8% lower than the center value. The other two capsules showed maximum and minimum varviations that were about 30% less than those of capsule B. The azimuthal variation is on the order of the measurement standard deviation and is substantially less than the observed bias in the RAMA predictions. As a result, the uncertainty in wire position in the capsules is relatively insignificant.

3.4.1 SSP Capsule A Activation Comparison Results

Content Deleted -
EPRI Proprietary Information

Table 3-8
Comparison of Specific Activities for Cooper Nuclear Station SSP Capsule A Flux Wires

Content Deleted -
EPRI Proprietary Information

Table 3-9
Comparison of Specific Activities for Cooper Nuclear Station SSP Capsule A Dosimetry

Content Deleted -
EPRI Proprietary Information

3.4.2 SSP Capsule B Activation Comparison Results

Content Deleted -
EPRI Proprietary Information

Table 3-10
Comparison of Specific Activities for Cooper Nuclear Station SSP Capsule B Flux Wires

Content Deleted -
EPRI Proprietary Information

Table 3-11
Comparison of Specific Activities for Cooper Nuclear Station SSP Capsule B Dosimetry

Content Deleted -
EPRI Proprietary Information

3.4.3 SSP Capsule C Activation Comparison Results

Content Deleted -
EPRI Proprietary Information

Table 3-12
Comparison of Specific Activities for Cooper Nuclear Station SSP Capsule C Flux Wires

Content Deleted -
EPRI Proprietary Information

Table 3-13
Comparison of Specific Activities for Cooper Nuclear Station SSP Capsule C Dosimetry

Content Deleted -
EPRI Proprietary Information

3.5 Surveillance Capsule Fluence Results

The best estimate neutron fluence and rated power neutron flux for each of the capsule specimen locations are provided below. Neutron fluence and flux values are provided for >1.0 MeV and >0.1 MeV. The best estimate fluence and flux values are determined by multiplying the RAMA-calculated fluence and flux by the appropriate multiplicative bias factor for each capsule from Section 3.4.

3.5.1 Surveillance Capsule Best Estimate Neutron Fluence and Flux for Energy >1.0 MeV

Tables 3-14 through 3-16 show the best estimate >1.0 MeV neutron fluence and flux at rated thermal power for SSP capsule A, B and C specimen locations, respectively.

Table 3-14
Best Estimate >1.0 MeV Neutron Fluence and Rated Power Flux in SSP Capsule A

Content Deleted -
EPRI Proprietary Information

Table 3-15
Best Estimate >1.0 MeV Neutron Fluence and Rated Power Flux in SSP Capsule B

Content Deleted -
EPRI Proprietary Information

Table 3-16
Best Estimate >1.0 MeV Neutron Fluence and Rated Power Flux in SSP Capsule C

Content Deleted -
EPRI Proprietary Information

3.5.2 Surveillance Capsule Best Estimate Neutron Fluence and Flux for Energy >0.1 MeV

Tables 3-17 through 3-19 show the best estimate >0.1 MeV neutron fluence and flux at rated thermal power for SSP capsule A, B and C specimen locations, respectively. The same bias factors used to determine the >1.0 MeV fluence and flux in Section 3.5.1 are assumed to be applicable to the determination of the best estimate >0.1 MeV fluence and flux as well.

Table 3-17
Best Estimate >0.1 MeV Neutron Fluence and Rated Power Flux in SSP Capsule A

Content Deleted -
EPRI Proprietary Information

Table 3-18
Best Estimate >0.1 MeV Neutron Fluence and Rated Power Flux in SSP Capsule B

Content Deleted -
EPRI Proprietary Information

Table 3-19
Best Estimate >0.1 MeV Neutron Fluence and Rated Power Flux in SSP Capsule C

Content Deleted -
EPRI Proprietary Information

4
CHARPY TEST DATA

4.1 Charpy Test Procedure

Charpy impact tests were conducted in accordance with ASTM Standards E 185-82 and E 23-02. A drawing showing the Charpy test specimen geometry is given in Figure 4-1. The 1982 version of E 185 has been reviewed and approved by NRC for surveillance capsule testing applications. This standard references ASTM E 23. The tests were conducted using a Tinius Olsen Testing Machine Company, Inc. Model 84 impact test machine with a 300 ft-lb (406.75 J) range. The Model 84 is equipped with a dial gage as well as the MPM optical encoder system for accurate absorbed energy measurement. In all cases, the optical encoder measured energy was reported as the impact energy because it is much more accurate than the dial. The optical encoder can resolve the energy to within 0.04 ft-lbs (0.054 J), whereas, for the dial, the resolution is around 0.25 ft-lbs (0.34 J). Therefore, because of the lower accuracy of the dial, and because of the fact that the pendulum was re-weighted to bring the center-of-percussion into close agreement with the center-of-strike, the dial energies were not recorded. The impact energy was corrected for windage and friction for each test performed using the optical encoder measurements. The velocity of the striker at impact was nominally 18 ft/s (5.49 m/s). The encoder system measures the exact impact velocity for every test. Calibration of the machine was verified as specified in E 23 and verification specimens were provided by NIST.

The E 23 procedure for specimen temperature control using an in-situ heating and cooling system was followed. Each specimen was held at the desired test temperature for at least 5 minutes prior to testing and the fracture process zone temperature was held to within ± 1.8 F (± 1 C) up to the instant of strike. Precision calibrated tongs were used for specimen centering on the test machine.

Lateral expansion (LE) was determined from measurements made with a lateral expansion gage. The lateral expansion gage was calibrated using precision gage blocks which are traceable to NIST. The percentage of shear fracture area was determined by integrating the ductile and brittle fracture areas.

The number of Charpy specimens for measurement of the transition region and upper shelf was limited. Therefore, the choice of test temperatures was very important. Prior to testing, the Charpy energy-temperature curve was predicted using fits of the unirradiated data. The first test was then conducted near the middle of the transition region and test temperature decisions were then made based on the test results. Overall, the goal was to perform three tests on the upper shelf and to use the remaining seven specimens to characterize the 30 ft-lb (41 J) index. This approach was successful as illustrated in the next report section.

4.2 Charpy Test Data

A total of 120 irradiated base metal and 120 irradiated weld specimens were tested over the transition region temperature range and on the upper shelf. As shown in Table 2-2, each capsule contained 8 material types (4 base metal and 4 weld), with a total of 10 Charpy specimens for each material type. The irradiated data are summarized in Appendix A, Tables A-1 through A-24. As discussed in [8] and [9], the base metal surveillance specimens have a T-L orientation. In addition to the energy absorbed by the specimen during impact, the measured lateral expansion values and the percentage shear fracture area for each test specimen are listed in the tables. The Charpy energy was read from the optical encoder and has been corrected for windage and friction in accordance with ASTM E 23. The optical encoder and the dial cannot correct for tossing energy and therefore this small amount of additional energy, if present, may be included in the data for some tests.

The lateral expansion is a measure of the transverse plastic deformation produced by the striking edge of the striker during the impact event. Lateral expansion is determined by measuring the maximum change of specimen thickness along the sides of the specimen. Lateral expansion is a measure of the ductility of the specimen. The nuclear industry tracks the embrittlement shift using the 35 mil (0.89 mm) lateral expansion index. In accordance with ASTM E23, the lateral expansion for some specimens, which could be broken after the impact test, should not be reported as broken since the lateral expansion of the unbroken specimen is less than that for the broken specimen. Therefore, when these conditions exist, the value listed in the table is the unbroken measurement and a footnote is included to identify these specimens.

The percentage of shear fracture area is a direct quantification of the transition in the fracture modes as the temperature increases. All metals with a body centered cubic lattice structure, such as ferritic pressure vessel materials, undergo a transition in fracture modes. At low test temperatures, a crack propagates in a brittle manner and cleaves across the grains. As the test temperature increases, the percentage of shear (or ductile) fracture increases. This temperature range is referred to as the transition region and the fracture process is mixed mode. As the temperature increases further, the fracture process is eventually completely ductile (i.e., no brittle component), and this temperature range is referred to as the upper shelf region.

Preparation of P-T operating curves requires the determination of the Charpy 30 ft-lb (41 J) transition temperature shift. This index is determined by fitting the energy-temperature data to find the mean curve. It is also necessary to estimate the upper shelf energy to ensure that the shelf has not dropped below the 10CFR50, Appendix G, 50 ft-lb (68 J) screening criterion. The Charpy data analysis results are provided in the next section of this report. 10CFR50, Appendix H requires that the unirradiated data be included in the surveillance report. Therefore, the base and weld unirradiated data are given in Appendix A, Tables A-25 through A-40.

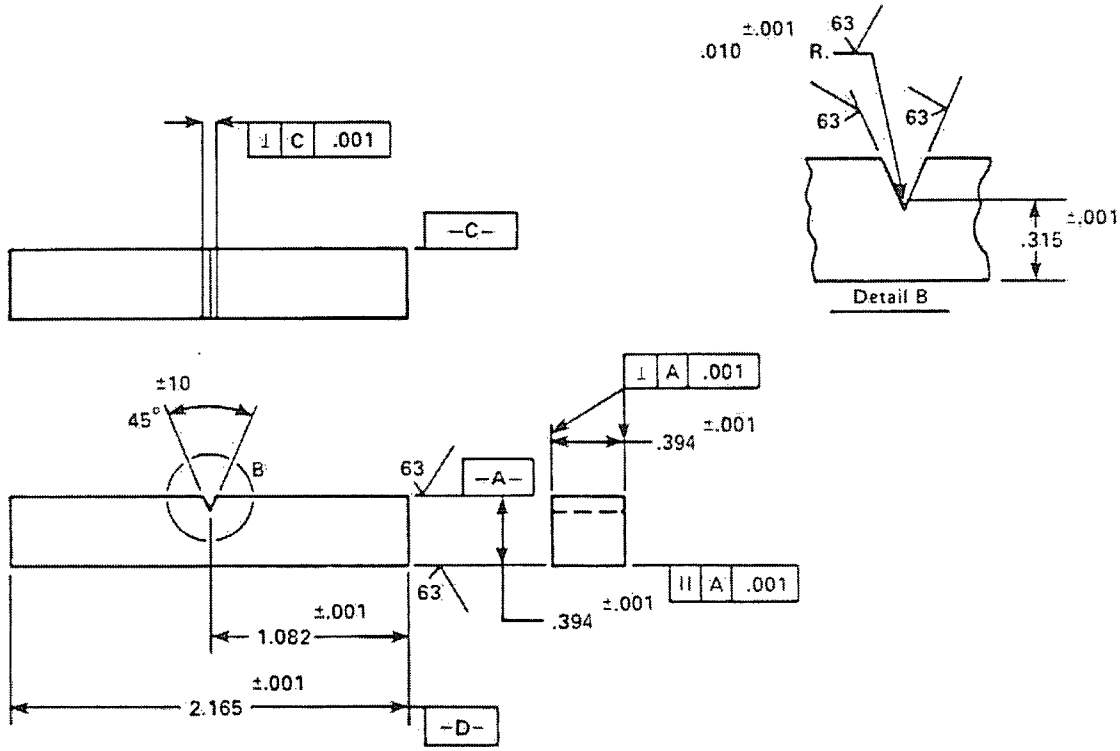

Table 4-1
Drawing Showing the Charpy Test Specimen Geometry.

5
CHARPY TEST RESULTS

5.1 Analysis of Impact Test Results

For analysis of the Charpy test data, the BWRVIP ISP has selected the hyperbolic tangent (tanh) function as the statistical curve-fit tool to model the transition temperature toughness data. A hyperbolic tangent curve-fitting program named CVGRAPH [10] developed by ATI Consulting was used to fit the Charpy V-notch energy and lateral expansion data. The impact energy curve-fits from CVGRAPH are provided in Appendix B. Lower shelf energy was fixed at 2.5 ft-lbs (3.4 J) in all cases, consistent with the methodology established for analysis of all ISP Charpy energy data [7]. Upper shelf energy was fixed at the average of all test energies (at least 3) exhibiting shear greater than or equal to 95%, consistent with ASTM Standard E185-82 [3]. In cases where there were not three data points exhibiting greater than 95% shear, an engineering judgment was made whether the upper shelf should remain free or be fixed at the average of those points with greater than 95% shear.

5.2 Irradiated Versus Unirradiated CVN Properties

Tables 5-1, 5-2, and 5-3 summarize the T_{30} [30 ft-lb (41 J) Transition Temperature], T_{50} [50 ft-lb (68 J) Transition Temperature], T_{35mil} [35 mil (0.89 mm) Lateral Expansion Temperature], and Upper Shelf Energy for the unirradiated and irradiated materials and show the change from baseline values for Capsules A, B, and C, respectively. These tables have been sequenced by capsule. The unirradiated and irradiated values are taken from the CVGRAPH fits provided in Appendix B.

Table 5-1
Effect of Irradiation (E>1.0 MeV) on the Notch Toughness Properties of Capsule A Materials

Material Identity[1]	T_{30}, 30 ft-lb (41 J) Transition Temperature			T_{35mil}, 35 mil (0.89 mm) Lateral Expansion Temperature			T_{50}, 50 ft-lb (68 J) Transition Temperature			CVN Upper Shelf Energy (USE)		
	Unirrad °F (°C)	Irradiated °F (°C)	ΔT_{30} °F (°C)	Unirrad °F (°C)	Irradiated °F (°C)	ΔT_{35mil} °F (°C)	Unirrad °F (°C)	Irradiated °F (°C)	ΔT_{50} °F (°C)	Unirrad ft-lb (J)	Irradiated ft-lb (J)	Change ft-lb (J)
A1224-1	-20.9 (-29.4)	0.3 (-17.6)	21.2 (11.8)	10.9 (-11.7)	9.7 (-12.4)	-1.2 (-0.7)	5.9 (-14.5)	20.6 (-6.3)	14.7 (8.2)	147.3 (199.7)	148.7 (201.6)	1.4 (1.9)
C2331-2	-13.3 (-25.2)	28.2 (-2.1)	41.5 (23.1)	34.1 (1.2)	44.4 (6.9)	10.3 (5.7)	30.1 (-1.1)	77.9 (25.5)	47.8 (26.6)	100.0 (135.6)	91.0 (123.4)	-9.0 (-12.2)
P2130-2	-2.8 (-19.3)	37.4 (3.0)	40.2 (22.3)	22.8 (-5.1)	58.9 (14.9)	36.1 (20.1)	41.6 (5.3)	89.1 (31.7)	47.5 (26.4)	68.2 (92.5)	63.9 (86.6)	-4.3 (-5.8)
C3278-2	-34.4 (-36.9)	-4.5 (-20.3)	29.9 (16.6)	15.1 (-9.4)	18.6 (-7.4)	3.5 (1.9)	5.4 (-14.8)	31.6 (-0.2)	26.2 (14.6)	113.3 (153.6)	103.3 (140.1)	-10.0 (-13.6)
5P6214B	-26.8 (-32.7)	-53.2 (-47.3)	-26.4 (-14.7)	9.2 (-12.7)	-18.8 (-28.2)	-28.0 (-15.6)	7.0 (-13.9)	-9.3 (-22.9)	-16.3 (-9.1)	91.5 (124.1)	96.5 (130.8)	5.0 (6.8)
34B009	-65.0 (-53.9)	34.0 (1.1)	99.0 (55.0)	-21.0 (-29.4)	67.3 (19.6)	88.3 (49.1)	-29.5 (-34.2)	92.7 (33.7)	122.2 (67.9)	104.4 (141.5)	92.1 (124.9)	-12.3 (-16.7)
Quad Cities 2 ESW	-23.1 (-30.6)	-10.4 (-23.6)	12.7 (7.1)	22.4 (-5.3)	27.7 (-2.4)	5.3 (2.9)	17.9 (-7.8)	45.3 (7.4)	27.4 (15.2)	104.0 (141.0)	100.7 (136.5)	-3.3 (-4.5)
406L44	-8.8 (-22.7)	113.1 (45.1)	121.9 (67.7)	39.2 (4.0)	171.5 (77.5)	132.3 (73.5)	51.1 (10.6)	223.9 (106.6)	172.8 (96.0)	73.3 (99.4)	58.3 (79.0)	-15.0 (-20.3)

Fluence is unique to each specimen set:
A1224-1 = 3.80×10^{17} n/cm^2 C2331-2 = 3.82×10^{17} n/cm^2 P2130-2 = 3.78×10^{17} n/cm^2 C3278-2 = 3.74×10^{17} n/cm^2
5P6214B = 4.09×10^{17} n/cm^2 34B009 = 4.08×10^{17} n/cm^2 QC2 ESW = 4.06×10^{17} n/cm^2 406L44 = 3.97×10^{17} n/cm^2

Table 5-2
Effect of Irradiation (E>1.0 MeV) on the Notch Toughness Properties of Capsule B Materials

Material Identity[1]	T_{30}, 30 ft-lb (41 J) Transition Temperature			T_{35mil}, 35 mil (0.89 mm) Lateral Expansion Temperature			T_{50}, 50 ft-lb (68 J) Transition Temperature			CVN Upper Shelf Energy (USE)		
	Unirrad °F (°C)	Irradiated °F (°C)	ΔT_{30} °F (°C)	Unirrad °F (°C)	Irradiated °F (°C)	ΔT_{35mil} °F (°C)	Unirrad °F (°C)	Irradiated °F (°C)	ΔT_{50} °F (°C)	Unirrad ft-lb (J)	Irradiated ft-lb (J)	Change ft-lb (J)
A1224-1	-20.9 (-29.4)	-27.7 (-33.2)	-6.8 (-3.8)	10.9 (-11.7)	-14.7 (-25.9)	-25.6 (-14.2)	5.9 (-14.5)	-0.4 (-18.0)	-6.3 (-3.5)	147.3 (199.7)	160.4 (217.5)	13.1 (17.8)
C2331-2	-13.3 (-25.2)	21.4 (-5.9)	34.7 (19.3)	34.1 (1.2)	39.2 (4.0)	5.1 (2.8)	30.1 (-1.1)	62.5 (16.9)	32.4 (18.0)	100.0 (135.6)	97.7 (132.5)	-2.3 (-3.1)
P2130-2	-2.8 (-19.3)	50.6 (10.3)	53.4 (29.7)	22.8 (-5.1)	69.9 (21.1)	47.1 (26.2)	41.6 (5.3)	101.0 (38.3)	59.4 (33.0)	68.2 (92.5)	67.7 (91.8)	-0.5 (-0.7)
C3278-2	-34.4 (-36.9)	8.5 (-13.1)	42.9 (23.8)	15.1 (-9.4)	31.1 (-0.5)	16.0 (8.9)	5.4 (-14.8)	50.1 (10.1)	44.7 (24.8)	113.3 (153.6)	100.4 (136.1)	-12.9 (-17.5)
5P6214B	-26.8 (-32.7)	-11.1 (-23.9)	15.7 (8.7)	9.2 (-12.7)	11.7 (-11.3)	2.5 (1.4)	7.0 (-13.9)	19.8 (-6.8)	12.8 (7.1)	91.5 (124.1)	97.4 (132.1)	5.9 (8.0)
34B009	-65.0 (-53.9)	35.6 (2.0)	100.6 (55.9)	-21.0 (-29.4)	70.2 (21.2)	91.2 (50.7)	-29.5 (-34.2)	81.9 (27.7)	111.4 (61.9)	104.4 (141.5)	98.8 (134.0)	-5.6 (-7.6)
Quad Cities 2 ESW	-23.1 (-30.6)	-11.9 (-24.4)	11.2 (6.2)	22.4 (-5.3)	19.4 (-7.0)	-3.0 (-1.7)	17.9 (-7.8)	31.8 (-0.1)	13.9 (7.7)	104.0 (141.0)	110.1 (149.3)	6.1 (8.3)
406L44	-8.8 (-22.7)	111.8 (44.3)	120.6 (67.0)	39.2 (4.0)	179.2 (81.8)	140.0 (77.8)	51.1 (10.6)	233.0 (111.7)	181.9 (101.1)	73.3 (99.4)	58.2 (78.9)	-15.1 (-20.5)

Fluence is unique to each specimen set:
A1224-1 = 4.90×10^{17} n/cm^2 C2331-2 = 4.79×10^{17} n/cm^2 P2130-2 = 4.68×10^{17} n/cm^2 C3278-2 = 4.54×10^{17} n/cm^2
5P6214B = 5.26×10^{17} n/cm^2 34B009 = 5.17×10^{17} n/cm^2 QC2 ESW = 5.04×10^{17} n/cm^2 406L44 = 4.93×10^{17} n/cm^2

Table 5-3
Effect of Irradiation (E>1.0 MeV) on the Notch Toughness Properties of Capsule C Materials

Material Identity[1]	T_{30}, 30 ft-lb (41 J) Transition Temperature			T_{35mil}, 35 mil (0.89 mm) Lateral Expansion Temperature			T_{50}, 50 ft-lb (68 J) Transition Temperature			CVN Upper Shelf Energy (USE)		
	Unirrad °F (°C)	Irradiated °F (°C)	ΔT_{30} °F (°C)	Unirrad °F (°C)	Irradiated °F (°C)	ΔT_{35mil} °F (°C)	Unirrad °F (°C)	Irradiated °F (°C)	ΔT_{50} °F (°C)	Unirrad ft-lb (J)	Irradiated ft-lb (J)	Change ft-lb (J)
C3985-2	-11.7 (-24.3)	8.8 (-12.9)	20.5 (11.4)	31.1 (-0.5)	30.6 (-0.8)	-0.5 (-0.3)	27.0 (-2.8)	46.4 (8.0)	19.4 (10.8)	112.8 (152.9)	115.8 (157.0)	3.0 (4.1)
C1079-1	9.7 (-12.4)	75.1 (23.9)	65.4 (36.3)	57.1 (13.9)	106.7 (41.5)	49.6 (27.6)	76.6 (24.8)	165.2 (74.0)	88.6 (49.2)	61.2 (83.0)	57.9 (78.5)	-3.3 (-4.5)
A0610-1	-33.5 (-36.4)	12.5 (-10.8)	46.0 (25.6)	-1.5 (-18.6)	39.5 (4.2)	41.0 (22.8)	-4.1 (-20.1)	57.6 (14.2)	61.7 (34.3)	101.2 (137.2)	98.8 (134.0)	-2.4 (-3.3)
A1195-1	39.8 (4.3)	64.9 (18.3)	25.1 (13.9)	79.6 (26.4)	93.7 (34.3)	14.1 (7.8)	78.7 (25.9)	108.7 (42.6)	30.0 (16.7)	99.7 (135.2)	104.1 (141.1)	4.4 (6.0)
20291	-17.8 (-27.7)	55.2 (12.9)	73.0 (40.6)	10.8 (-11.8)	81.6 (27.6)	70.8 (39.3)	13.3 (-10.4)	88.7 (31.5)	75.4 (41.9)	110.0 (149.1)	93.6 (126.9)	-16.4 (-22.2)
B&W Linde 80 SAW	40.0 (4.4)	125.5 (51.9)	85.5 (47.5)	80.9 (27.2)	170.9 (77.2)	90.0 (50.0)	94.9 (34.9)	217.2 (102.9)	122.3 (67.9)	75.8 (102.8)	64.7 (87.7)	-11.1 (-15.0)
Humboldt Bay 3 SAW	-74.0 (-58.9)	-15.7 (-26.5)	58.3 (32.4)	-24.6 (-31.4)	18.3 (-7.6)	42.9 (23.8)	-29.3 (-34.1)	32.4 (0.2)	61.7 (34.3)	110.3 (149.5)	99.7 (135.2)	-10.6 (-14.4)
5P6756	-67.1 (-55.1)	-43.5 (-41.9)	23.6 (13.1)	-20.3 (-29.1)	-17.4 (-27.4)	2.9 (1.6)	-21.3 (-29.6)	0.7 (-17.4)	22.0 (12.2)	104.4 (141.5)	110.7 (150.1)	6.3 (8.5)

Fluence is unique to each specimen set:
C3985-2 = 3.11×10^{17} n/cm^2 C1079-1 = 3.02×10^{17} n/cm^2 A0610-1 = 2.93×10^{17} n/cm^2 A1195-1 = 2.79×10^{17} n/cm^2
20291 = 3.29×10^{17} n/cm^2 B&W Linde 80 SAW = 3.22×10^{17} n/cm^2 Humboldt Bay 3 SAW = 3.13×10^{17} n/cm^2 5P6756 = 2.93×10^{17} n/cm^2

The materials irradiated in SSP (Cooper) capsules A, B, and C exhibited a wide range of embrittlement sensitivity. All but seven of the materials experienced less embrittlement than predicted using [6] (including margin), based on a unique fluence (E > 1.0 MeV) for each set of specimens. Tables 5-4, 5-5, and 5-6 illustrate this comparison for Capsules A, B, and C, respectively. Measured shifts that are greater than predicted shifts (including margin) are shown in bold.

Measured percent decreases in USE are presented in Tables 5-7, 5-8, and 5-9. Note that a negative decrease means an actual increase in the USE.

Table 5-4
Comparison of Actual Versus Predicted Embrittlement of SSP Capsule A Materials

Content Deleted -
EPRI Proprietary Information

Table 5-5
Comparison of Actual Versus Predicted Embrittlement of SSP Capsule B Materials

Content Deleted -
EPRI Proprietary Information

Table 5-6
Comparison of Actual Versus Predicted Embrittlement of SSP Capsule C Materials

Content Deleted -
EPRI Proprietary Information

Table 5-7
Percent Decrease in Upper Shelf Energy (USE) of SSP Capsule A Materials

Content Deleted -
EPRI Proprietary Information

Table 5-8
Percent Decrease in Upper Shelf Energy (USE) of SSP Capsule B Materials

Content Deleted -
EPRI Proprietary Information

Table 5-9
Percent Decrease in Upper Shelf Energy (USE) of SSP Capsule C Materials

Content Deleted -
EPRI Proprietary Information

6
REFERENCES

1. 10 CFR 50, Appendices G (*Fracture Toughness Requirements*) and H (*Reactor Vessel Material Surveillance Program Requirements*), Federal Register, Volume 60, No. 243, dated December 19, 1995.

2. *Fracture Toughness Criteria for Protection Against Failure*, Appendix G to Section III or XI of the ASME Boiler & Pressure Vessel Code, 1995 Edition with addenda through 1996 Addenda.

3. ASTM E185-82, *Standard Practice for Conducting Surveillance Tests for Light-Water Cooled Nuclear Power Reactor Vessels*, E706 (IF), ASTM Standards, Section 3, American Society for Testing and Materials, Philadelphia, PA, 1993.

4. GE Report, GE-NE-523-101-1290, "Progress Report on Phase 2 of the BWR Owners' Group Supplemental Surveillance Program," January, 1992.

5. BWRVIP-86-A: BWR Vessel and Internals Project, "Updated BWR Integrated Surveillance Program Implementation Plan," EPRI Technical Report 1003346, October 2002.

6. U.S. NRC Regulatory Guide 1.99, "Radiation Embrittlement of Reactor Vessel Materials," Revision 2, May 1988.

7. BWRVIP-135: BWR Vessel and Internal Project Integrated Surveillance Program (ISP) Data Source Book and Plant Evaluations, EPRI, Palo Alto, CA: 2004. 1011019.

8. GE Report GE-NE-523-79-0791, "Baseline Charpy and Chemistry Data for Materials Used in the BWR Owners' Group Supplemental Surveillance Program," September, 1991.

9. GE Nuclear Letter B11-00834-00-LT02R1, to ATI Consulting, May 11, 2000

10. CVGRAPH, Hyperbolic Tangent Curve Fitting Program, Developed by ATI Consulting, Version 5.0.2, Revision 1, 3/26/02.

11. Wang, M.T., "Fracture Toughness of RPV Steel Welds," GE Report NEDC-30299, October 1983.

12. "Calculational and Dosimetry Methods for Determining Pressure Vessel Neutron Fluence," Nuclear Regulatory Commission Regulatory Guide 1.190, March 2001.

13. Nebraska Public Power District Calculation Number NEDC 04-018, "RPV Fluence Mechanical Design Inputs," April 30, 2004.

14. Nebraska Public Power District Calculation Number NEDC 04-019, "Cycle 1 to 21 Design Inputs for RAMA Fluence Analysis," July 23, 2004.

15. BWRVIP-126: BWR Vessel Internals Project, RAMA Fluence Methodology Software, Version 1.0, EPRI, Palo Alto, CA: 2003. 1007823.

16. BWRVIP-114: BWR Vessel Internals Project, RAMA Fluence Methodology Theory Manual, EPRI, Palo Alto, CA: 2003. 1003660.

17. BWRVIP-121: BWR Vessel Internals Project, RAMA Fluence Methodology Procedures Manual, EPRI, Palo Alto, CA: 2003. 1008062.

18. "Letter from William H. Bateman (U. S. NRC) to Bill Eaton (BWRVIP), "Safety Evaluation of Proprietary EPRI Reports BWRVIP-114, -115, -117, and -121 and TWE-PSE-001-R-001," dated May 13, 2005.

19. BWRVIP-115: BWR Vessel and Internals Project, RAMA Fluence Methodology Benchmark Manual – Evaluation of Regulatory Guide 1.190 Benchmark Problems, EPRI, Palo Alto, CA: 2003 1008063.

20. "BUGLE-96: Coupled 47 Neutron, 20 Gamma-Ray Group Cross Section Library Derived from ENDF/B-VI for LWR Shielding and Pressure Vessel Dosimetry Applications," RSICC Data Library Collection, DLC-185, March 1996.

A
SUMMARY OF CHARPY V-NOTCH TEST DATA

Table A-1
Charpy V-Notch Results for Capsule A Plate A1224-1

Content Deleted -
EPRI Proprietary Information

Table A-2
Charpy V-Notch Results for Capsule A Plate Heat C2331-2

Content Deleted -
EPRI Proprietary Information

Table A-3
Charpy V-Notch Results for Capsule A Plate Heat P2130-2

Content Deleted -
EPRI Proprietary Information

Table A-4
Charpy V-Notch Results for Capsule A Plate Heat C3278-2

Content Deleted -
EPRI Proprietary Information

Table A-5
Charpy V-Notch Results for Capsule A Weld Heat 5P6214B

Content Deleted -
EPRI Proprietary Information

Table A-6
Charpy V-Notch Results for Capsule A Weld Heat 34B009

Content Deleted -
EPRI Proprietary Information

Table A-7
Charpy V-Notch Results for Capsule A Quad Cities 2 Electroslag Weld (Heat unknown)

Content Deleted -
EPRI Proprietary Information

Table A-8
Charpy V-Notch Results for Capsule A Weld Heat 406L44

Content Deleted -
EPRI Proprietary Information

Table A-9
Charpy V-Notch Results for Capsule B Plate Heat A1224-1

Content Deleted -
EPRI Proprietary Information

Table A-10
Charpy V-Notch Results for Capsule B Plate Heat C2331-2

Content Deleted -
EPRI Proprietary Information

Table A-11
Charpy V-Notch Results for Capsule B Plate Heat P2130-2

Content Deleted -
EPRI Proprietary Information

Table A-12
Charpy V-Notch Results for Capsule B Plate Heat C3278-2

Content Deleted -
EPRI Proprietary Information

Table A-13
Charpy V-Notch Results for Capsule B Weld Heat 5P6214B

Content Deleted -
EPRI Proprietary Information

Table A-14
Charpy V-Notch Results for Capsule B Weld Heat 34B009

Content Deleted -
EPRI Proprietary Information

Table A-15
Charpy V-Notch Results for Capsule B Quad Cities 2 Electroslag Weld (Heat unknown)

Content Deleted -
EPRI Proprietary Information

Table A-16
Charpy V-Notch Results for Capsule B Weld Heat 406L44

Content Deleted -
EPRI Proprietary Information

Table A-17
Charpy V-Notch Results for Capsule C Plate Heat C3985-2

Content Deleted -
EPRI Proprietary Information

Table A-18
Charpy V-Notch Results for Capsule C Plate Heat C1079-1

Content Deleted -
EPRI Proprietary Information

Table A-19
Charpy V-Notch Results for Capsule C Plate Heat A0610-1

Content Deleted -
EPRI Proprietary Information

Table A-20
Charpy V-Notch Results for Capsule C Plate HSST-02 Heat A1195-1

Content Deleted -
EPRI Proprietary Information

Table A-21
Charpy V-Notch Results for Capsule C Weld Heat 20291

Content Deleted -
EPRI Proprietary Information

Table A-22
Charpy V-Notch Results for Capsule C B&W Linde 80 Weld (Heat unknown)

Content Deleted -
EPRI Proprietary Information

Table A-23
Charpy V-Notch Results for Capsule C Humboldt Bay 3 Weld (Heat unknown)

Content Deleted -
EPRI Proprietary Information

Table A-24
Charpy V-Notch Results for Capsule C Weld Heat 5P6756

Content Deleted -
EPRI Proprietary Information

Table A-25
Charpy V-Notch Results for Unirradiated SSP Plate Heat A1224-1

Content Deleted -
EPRI Proprietary Information

Table A-26
Charpy V-Notch Results for Unirradiated SSP Plate Heat C2331-2

Content Deleted -
EPRI Proprietary Information

Table A-27
Charpy V-Notch Results for Unirradiated SSP Plate Heat P2130-2

Content Deleted -
EPRI Proprietary Information

Table A-28
Charpy V-Notch Results for Unirradiated SSP Plate Heat C3278-2

Content Deleted -
EPRI Proprietary Information

Table A-29
Charpy V-Notch Results for Unirradiated SSP Plate Heat C3985-2

Content Deleted -
EPRI Proprietary Information

Table A-30
Charpy V-Notch Results for Unirradiated SSP Plate Heat C1079-1

Content Deleted -
EPRI Proprietary Information

Table A-31
Charpy V-Notch Results for Unirradiated SSP Plate Heat A0610-1

Content Deleted -
EPRI Proprietary Information

Table A-32
Charpy V-Notch Results for Unirradiated SSP Heat A1195-1

Content Deleted -
EPRI Proprietary Information

Table A-33
Charpy V-Notch Results for Unirradiated SSP Weld 5P6214B

Content Deleted -
EPRI Proprietary Information

Table A-34
Charpy V-Notch Results for Unirradiated SSP Weld 34B009

Content Deleted -
EPRI Proprietary Information

Table A-35
Charpy V-Notch Results for Unirradiated SSP Quad Cities 2 Electroslag Weld (Heat unknown)

Content Deleted -
EPRI Proprietary Information

Table A-36
Charpy V-Notch Results for Unirradiated SSP Weld 406L44

Content Deleted -
EPRI Proprietary Information

Table A-37
Charpy V-Notch Results for Unirradiated SSP Weld 20291

Content Deleted -
EPRI Proprietary Information

Table A-38
Charpy V-Notch Results for Unirradiated SSP B&W Linde 80 Weld (Heat unknown)

Content Deleted -
EPRI Proprietary Information

Table A-39
Charpy V-Notch Results for Unirradiated SSP Humboldt Bay Weld (Heat unknown)

Content Deleted -
EPRI Proprietary Information

Table A-40
Charpy V-Notch Results for Unirradiated SSP Weld 5P6756

Content Deleted -
EPRI Proprietary Information

B
TANH CURVE FIT PLOTS OF CVN TEST DATA

Content Deleted -
EPRI Proprietary Information

Content Deleted -
EPRI Proprietary Information

Figure B-1
Charpy Energy Data for A1224-1 Grand Gulf Plate Unirradiated

Content Deleted -
EPRI Proprietary Information

Figure B-1 (continued)
Charpy Energy Data for A1224-1 Grand Gulf Plate Unirradiated

Content Deleted -
EPRI Proprietary Information

Figure B-2
Charpy Energy Data for A1224-1 Grand Gulf Plate Irradiated in Capsule A

Content Deleted -
EPRI Proprietary Information

Figure B-2 (continued)
Charpy Energy Data for A1224-1 Grand Gulf Plate Irradiated in Capsule A

Content Deleted -
EPRI Proprietary Information

Figure B-3
Charpy Energy Data for A1224-1 Grand Gulf Plate Irradiated in Capsule B

Content Deleted -
EPRI Proprietary Information

Figure B-3 (continued)
Charpy Energy Data for A1224-1 Grand Gulf Plate Irradiated in Capsule B

Content Deleted -
EPRI Proprietary Information

Figure B-4
Charpy Energy Data for C2331-2 Cooper Plate Unirradiated

Content Deleted -
EPRI Proprietary Information

Figure B-4 (continued)
Charpy Energy Data for C2331-2 Cooper Plate Unirradiated

Content Deleted -
EPRI Proprietary Information

Figure B-5
Charpy Energy Data for C2331-2 Cooper Plate Irradiated in Capsule A

Content Deleted -
EPRI Proprietary Information

Figure B-5 (continued)
Charpy Energy Data for C2331-2 Cooper Plate Irradiated in Capsule A

Content Deleted -
EPRI Proprietary Information

Figure B-6
Charpy Energy Data for C2331-2 Cooper Plate Irradiated in Capsule B

Content Deleted -
EPRI Proprietary Information

Figure B-6 (continued)
Charpy Energy Data for C2331-2 Cooper Plate Irradiated in Capsule B

Content Deleted -
EPRI Proprietary Information

Figure B-7
Charpy Energy Data for P2130-2 Nine Mile Point 1 Plate Unirradiated

Content Deleted -
EPRI Proprietary Information

Figure B-7 (continued)
Charpy Energy Data for P2130-2 Nine Mile Point 1 Plate Unirradiated

Content Deleted -
EPRI Proprietary Information

Figure B-8
Charpy Energy Data for P2130-2 Nine Mile Point 1 Plate Irradiated in Capsule A

Content Deleted -
EPRI Proprietary Information

Figure B-8 (continued)
Charpy Energy Data for P2130-2 Nine Mile Point 1 Plate Irradiated in Capsule A

Content Deleted -
EPRI Proprietary Information

Figure B-9
Charpy Energy Data for P2130-2 Nine Mile Point 1 Plate Irradiated in Capsule B

Content Deleted -
EPRI Proprietary Information

Figure B-9 (continued)
Charpy Energy Data for P2130-2 Nine Mile Point 1 Plate Irradiated in Capsule B

Content Deleted -
EPRI Proprietary Information

Figure B-10
Charpy Energy Data for C3278-2 Fitzpatrick Plate Unirradiated

Content Deleted -
EPRI Proprietary Information

Figure B-10 (continued)
Charpy Energy Data for C3278-2 Fitzpatrick Plate Unirradiated

Content Deleted -
EPRI Proprietary Information

Figure B-11
Charpy Energy Data for C3278-2 Fitzpatrick Plate Irradiated in Capsule A

Content Deleted -
EPRI Proprietary Information

Figure B-11 (continued)
Charpy Energy Data for C3278-2 Fitzpatrick Plate Irradiated in Capsule A

Content Deleted -
EPRI Proprietary Information

Figure B-12
Charpy Energy Data for C3278-2 Fitzpatrick Plate Irradiated in Capsule B

Content Deleted -
EPRI Proprietary Information

Figure B-12 (continued)
Charpy Energy Data for C3278-2 Fitzpatrick Plate Irradiated in Capsule B

Content Deleted -
EPRI Proprietary Information

Figure B-13
Charpy Energy Data for 5P6214B Grand Gulf Weld Unirradiated

Content Deleted -
EPRI Proprietary Information

Figure B-13 (continued)
Charpy Energy Data for 5P6214B Grand Gulf Weld Unirradiated

Content Deleted -
EPRI Proprietary Information

Figure B-14
Charpy Energy Data for 5P6214B Grand Gulf Weld Irradiated in Capsule A

Content Deleted -
EPRI Proprietary Information

Figure B-14 (continued)
Charpy Energy Data for 5P6214B Grand Gulf Weld Irradiated in Capsule A

Content Deleted -
EPRI Proprietary Information

Figure B-15
Charpy Energy Data for 5P6214B Grand Gulf Weld Irradiated in Capsule B

Content Deleted -
EPRI Proprietary Information

Figure B-15 (continued)
Charpy Energy Data for 5P6214B Grand Gulf Weld Irradiated in Capsule B

Content Deleted -
EPRI Proprietary Information

Figure B-16
Charpy Energy Data for 34B009 Millstone 1 Weld Unirradiated

Content Deleted -
EPRI Proprietary Information

Figure B-16 (continued)
Charpy Energy Data for 34B009 Millstone 1 Weld Unirradiated

Content Deleted -
EPRI Proprietary Information

Figure B-17
Charpy Energy Data for 34B009 Millstone 1 Weld Irradiated in Capsule A

Content Deleted -
EPRI Proprietary Information

Figure B-17 (continued)
Charpy Energy Data for 34B009 Millstone 1 Weld Irradiated in Capsule A

Content Deleted -
EPRI Proprietary Information

Figure B-18
Charpy Energy Data for 34B009 Millstone 1 Weld Irradiated in Capsule B

Content Deleted -
EPRI Proprietary Information

Figure B-18 (continued)
Charpy Energy Data for 34B009 Millstone 1 Weld Irradiated in Capsule B

Content Deleted -
EPRI Proprietary Information

Figure B-19
Charpy Energy Data for AP2-21 Quad Cities 2 Weld Unirradiated

Content Deleted -
EPRI Proprietary Information

Figure B-19 (continued)
Charpy Energy Data for AP2-21 Quad Cities 2 Weld Unirradiated

Content Deleted -
EPRI Proprietary Information

Figure B-20
Charpy Energy Data for AP2-21 Quad Cities 2 Weld Irradiated in Capsule A

Content Deleted -
EPRI Proprietary Information

Figure B-20 (continued)
Charpy Energy Data for AP2-21 Quad Cities 2 Weld Irradiated in Capsule A

Content Deleted -
EPRI Proprietary Information

Figure B-21
Charpy Energy Data for BP2-21 Quad Cities 2 Weld Irradiated in Capsule B

Content Deleted -
EPRI Proprietary Information

Figure B-21 (continued)
Charpy Energy Data for BP2-21 Quad Cities 2 Weld Irradiated in Capsule B

Content Deleted -
EPRI Proprietary Information

Figure B-22
Charpy Energy Data for 406L44 Quad Cities 1 Weld Unirradiated

Content Deleted -
EPRI Proprietary Information

Figure B-22 (continued)
Charpy Energy Data for 406L44 Quad Cities 1 Weld Unirradiated

Content Deleted -
EPRI Proprietary Information

Figure B-23
Charpy Energy Data for 406L44 Quad Cities 1 Weld Irradiated in Capsule A

Content Deleted -
EPRI Proprietary Information

Figure B-23 (continued)
Charpy Energy Data for 406L44 Quad Cities 1 Weld Irradiated in Capsule A

Content Deleted -
EPRI Proprietary Information

Figure B-24
Charpy Energy Data for 406L44 Quad Cities 1 Weld Irradiated in Capsule B

Content Deleted -
EPRI Proprietary Information

Figure B-24 (continued)
Charpy Energy Data for 406L44 Quad Cities 1 Weld Irradiated in Capsule B

Content Deleted -
EPRI Proprietary Information

Figure B-25
Charpy Energy Data for C3985-2 Hatch 1 Plate Unirradiated

Content Deleted -
EPRI Proprietary Information

Figure B-25 (continued)
Charpy Energy Data for C3985-2 Hatch 1 Plate Unirradiated

Content Deleted -
EPRI Proprietary Information

Figure B-26
Charpy Energy Data for C3985-2 Hatch 1 Plate Irradiated in Capsule C

Content Deleted -
EPRI Proprietary Information

Figure B-26 (continued)
Charpy Energy Data for C3985-2 Hatch 1 Plate Irradiated in Capsule C

Content Deleted -
EPRI Proprietary Information

Figure B-27
Charpy Energy Data for C1079-1 Millstone 1 Plate Unirradiated

Content Deleted -
EPRI Proprietary Information

Figure B-27 (continued)
Charpy Energy Data for C1079-1 Millstone 1 Plate Unirradiated

Content Deleted -
EPRI Proprietary Information

Figure B-28
Charpy Energy Data for C1079-1 Millstone 1 Plate Irradiated in Capsule C

Content Deleted -
EPRI Proprietary Information

Figure B-28 (continued)
Charpy Energy Data for C1079-1 Millstone 1 Plate Irradiated in Capsule C

Content Deleted -
EPRI Proprietary Information

Figure B-29
Charpy Energy Data for A0610-1 Quad Cities 1 Plate Unirradiated

Content Deleted -
EPRI Proprietary Information

Figure B-29 (continued)
Charpy Energy Data for A0610-1 Quad Cities 1 Plate Unirradiated

Content Deleted -
EPRI Proprietary Information

Figure B-30
Charpy Energy Data for A0610-1 Quad Cities 1 Plate Irradiated in Capsule C

Content Deleted -
EPRI Proprietary Information

Figure B-30 (continued)
Charpy Energy Data for A0610-1 Quad Cities 1 Plate Irradiated in Capsule C

Content Deleted -
EPRI Proprietary Information

Figure B-31
Charpy Energy Data for A1195-1 HSST-02 Plate Unirradiated

Content Deleted -
EPRI Proprietary Information

Figure B-31 (continued)
Charpy Energy Data for A1195-1 HSST-02 Plate Unirradiated

Content Deleted -
EPRI Proprietary Information

Figure B-32
Charpy Energy Data for A1195-1 HSST-02 Plate Irradiated in Capsule C

Content Deleted -
EPRI Proprietary Information

Figure B-32 (continued)
Charpy Energy Data for A1195-1 HSST-02 Plate Irradiated in Capsule C

Content Deleted -
EPRI Proprietary Information

Figure B-33
Charpy Energy Data for Cooper Weld 20291 Unirradiated

Content Deleted -
EPRI Proprietary Information

Figure B-33 (continued)
Charpy Energy Data for Cooper Weld 20291 Unirradiated

Content Deleted -
EPRI Proprietary Information

Figure B-34
Charpy Energy Data for Cooper Weld 20291 Irradiated in Capsule C

Content Deleted -
EPRI Proprietary Information

Figure B-34 (continued)
Charpy Energy Data for Cooper Weld 20291 Irradiated in Capsule C

Content Deleted -
EPRI Proprietary Information

Figure B-35
Charpy Energy Data for AP2-BW B&W Linde 80 Weld Unirradiated

Content Deleted -
EPRI Proprietary Information

Figure B-35 (continued)
Charpy Energy Data for AP2-BW B&W Linde 80 Weld Unirradiated

Content Deleted -
EPRI Proprietary Information

Figure B-36
Charpy Energy Data for CP2-BW B&W Linde 80 Weld Irradiated in Capsule C

Content Deleted -
EPRI Proprietary Information

Figure B-36 (continued)
Charpy Energy Data for CP2-BW B&W Linde 80 Weld Irradiated in Capsule C

Content Deleted -
EPRI Proprietary Information

Figure B-37
Charpy Energy Data for CP2-6 Humboldt Bay 3 Weld Unirradiated

Content Deleted -
EPRI Proprietary Information

Figure B-37 (continued)
Charpy Energy Data for CP2-6 Humboldt Bay 3 Weld Unirradiated

Content Deleted -
EPRI Proprietary Information

Figure B-38
Charpy Energy Data for CP2-6 Humboldt Bay 3 Weld Irradiated in Capsule C

Content Deleted -
EPRI Proprietary Information

Figure B-38 (continued)
Charpy Energy Data for CP2-6 Humboldt Bay 3 Weld Irradiated in Capsule C

Content Deleted -
EPRI Proprietary Information

Figure B-39
Charpy Energy Data for 5P6756 River Bend Weld Unirradiated

Content Deleted -
EPRI Proprietary Information

Figure B-39 (continued)
Charpy Energy Data for 5P6756 River Bend Weld Unirradiated

Content Deleted -
EPRI Proprietary Information

Figure B-40
Charpy Energy Data for 5P6756 River Bend Weld Irradiated in Capsule C

Content Deleted -
EPRI Proprietary Information

Figure B-40 (continued)
Charpy Energy Data for 5P6756 River Bend Weld Irradiated in Capsule C

C
DOSIMETER ANALYSIS

Dosimeter Material Description

Content Deleted -
EPRI Proprietary Information

Dosimeter Cleaning and Mass Measurement

Content Deleted -
EPRI Proprietary Information

Content Deleted -
EPRI Proprietary Information

Radiometric Analysis

Content Deleted -
EPRI Proprietary Information

Content Deleted -
EPRI Proprietary Information

Table C-1
Cooper SSP Capsules A, B and C Wire Dosimeter Masses.

Content Deleted -
EPRI Proprietary Information

Table C-1 (continued)
Cooper SSP Capsules A, B and C Wire Dosimeter Masses.

Content Deleted -
EPRI Proprietary Information

Table C-2
Cooper SSP Capsules A, B and C Spectral Monitor Dosimeter Masses.

Content Deleted -
EPRI Proprietary Information

Table C-3
GRSS Specifications.

Content Deleted -
EPRI Proprietary Information

Table C-4
Counting Schedule for the Flux Wire Dosimeter Materials.

Content Deleted -
EPRI Proprietary Information

Table C-4 (continued)
Counting Schedule for the Flux Wire Dosimeter Materials.

Content Deleted -
EPRI Proprietary Information

Table C-5
Counting Schedule for the Spectral Monitor Dosimeter Materials.

Content Deleted -
EPRI Proprietary Information

Table C-6
Neutron-Induced Reactions of Interest.

Content Deleted -
EPRI Proprietary Information

Table C-7
Results of the Radiometric Analysis for the Flux Wires.

Content Deleted -
EPRI Proprietary Information

Table C-7 (continued)
Results of the Radiometric Analysis for the Flux Wires.

Content Deleted -
EPRI Proprietary Information

Table C-8
Results of the Radiometric Analysis for the Spectral Monitors.

Content Deleted -
EPRI Proprietary Information

Table C-8 (continued)
Results of the Radiometric Analysis for the Spectral Monitors.

Content Deleted -
EPRI Proprietary Information

Content Deleted -
EPRI Proprietary Information

Figure C-1
Schematic Representation of the SSP Capsule A Dosimetry Wire Layout Relative to the Charpy Test Specimens.

Content Deleted -
EPRI Proprietary Information

Figure C-2
Schematic Representation of the SSP Capsule B Dosimetry Wire Layout Relative to the Charpy Test Specimens.

Content Deleted -
EPRI Proprietary Information

Figure C-3
Schematic Representation of the SSP Capsule C Dosimetry Wire Layout Relative to the Charpy Test Specimens.

Export Control Restrictions

Access to and use of EPRI Intellectual Property is granted with the specific understanding and requirement that responsibility for ensuring full compliance with all applicable U.S. and foreign export laws and regulations is being undertaken by you and your company. This includes an obligation to ensure that any individual receiving access hereunder who is not a U.S. citizen or permanent U.S. resident is permitted access under applicable U.S. and foreign export laws and regulations. In the event you are uncertain whether you or your company may lawfully obtain access to this EPRI Intellectual Property, you acknowledge that it is your obligation to consult with your company's legal counsel to determine whether this access is lawful. Although EPRI may make available on a case-by-case basis an informal assessment of the applicable U.S. export classification for specific EPRI Intellectual Property, you and your company acknowledge that this assessment is solely for informational purposes and not for reliance purposes. You and your company acknowledge that it is still the obligation of you and your company to make your own assessment of the applicable U.S. export classification and ensure compliance accordingly. You and your company understand and acknowledge your obligations to make a prompt report to EPRI and the appropriate authorities regarding any access to or use of EPRI Intellectual Property hereunder that may be in violation of applicable U.S. or foreign export laws or regulations.

The Electric Power Research Institute (EPRI), with major locations in Palo Alto, California; Charlotte, North Carolina; and Knoxville, Tennessee, was established in 1973 as an independent, nonprofit center for public interest energy and environmental research. EPRI brings together members, participants, the Institute's scientists and engineers, and other leading experts to work collaboratively on solutions to the challenges of electric power. These solutions span nearly every area of electricity generation, delivery, and use, including health, safety, and environment. EPRI's members represent over 90% of the electricity generated in the United States. International participation represents nearly 15% of EPRI's total research, development, and demonstration program.

Together...Shaping the Future of Electricity

Program:

Nuclear Power

© 2007 Electric Power Research Institute (EPRI), Inc. All rights reserved. Electric Power Research Institute, EPRI, and TOGETHER...SHAPING THE FUTURE OF ELECTRICITY are registered service marks of the Electric Power Research Institute, Inc.

1013399NP

Electric Power Research Institute
3420 Hillview Avenue, Palo Alto, California 94304-1338 • PO Box 10412, Palo Alto, California 94303-0813 USA
800.313.3774 • 650.855.2121 • askepri@epri.com • www.epri.com